Mineral Exploration Targeting

eit RawMaterials Connecting matters

Funded by the European Union

eit RawMaterials ACADEMY

Indicator minerals analytical techniques: isotope and trace element analysis

GTK

UiT / Norges arktiske universitet

GEUS

AGH

University of Oulu

PALSATECH

CRS Laboratories

MAWSON

- Introduction on indicating minerals, analytical techniques and sample preparation
- Low precision isotope ratio:
  Trace element Fingerprinting by LA-ICPMS
- High precision isotope ratio by LA-MC-ICPMS:
  Which isotope for which mineral
  Which isotope for what purpose
- The use of isotopes in mineral exploration from examples
- The future

Indicating minerals associated with sulphide mineralisations

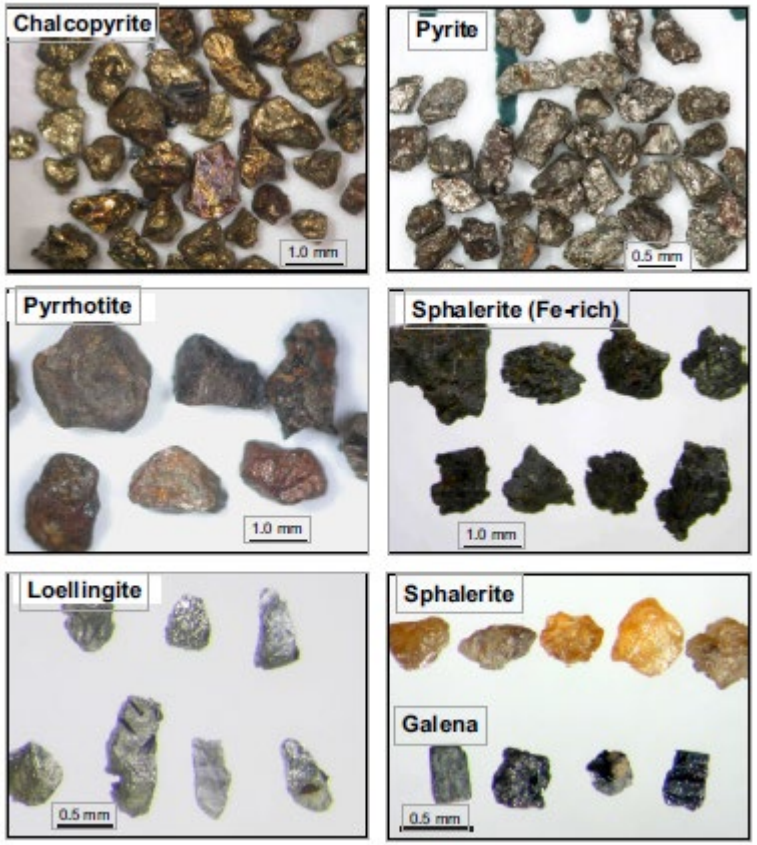

Mineral	Formula	Density
Tourmaline	Na,Ca)(Mg,Fe)$_3$Al6(**B**O$_3$)^3(Si$_6$O$_{18}$)(OH)^4	3.06
Loellingite	**Fe**As$_2$	7.1–7.7
Chalcopyrite	**CuFeS$_2$** **(Pb)**	4.1–4.3
Pyrite	**FeS$_2$**	5–5.02
Galena	**Pb**S	7.2–7.6
Sphalerite	**(Zn,Fe)S**	3.9–4.2
Pyrrhotite	**Fe**(1-x)S	4.58–4.65
Cassiterite	SnO$_2$ **(U-Pb)**	6.8–7.0

Photographs of selected VMS indicator minerals as they appear in heavy mineral concentrates of till from around VMS deposits. McClenaghan et al (2015)

Indicating minerals used in chemical stratigraphy study

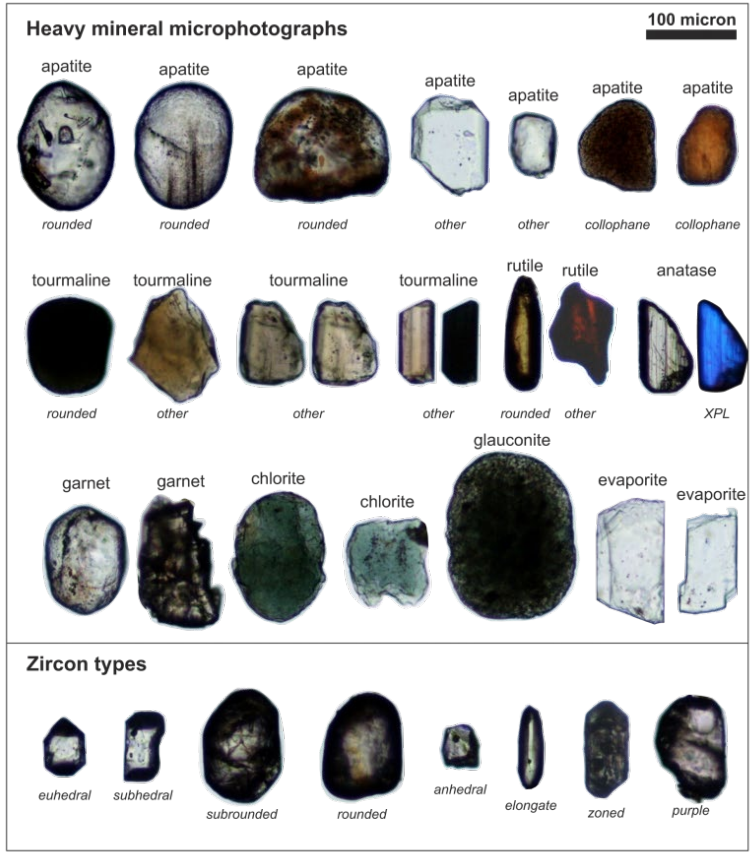

Fig. 2. Selected examples of heavy minerals and detrital zircon types from the Hansa oil field. XPL - microphotographs taken in crossed polarised light. All other microphotographs are in plane polarised light. Note that many rounded grains have pitted and frosted surfaces indicating sedimentary recycling.

https://www.chemostrat.com/heavy-minerals/

Minerals:

- Apatite ($Ca_5(PO_4)^3(F,Cl,OH)$) : U-Pb, Rb-Sr ρ= 3.2
- Zircon ($ZrSiO_4$): U-Pb, Lu-Hf ρ= 6.4
- Monazite $(Ce, La, Th)PO_4$: U-Pb, Sm-Nd ρ= 4.6-5.7
- Rutile (TiO2) U-Pb ρ= 4.3
- Tourmaline

  $(X_1Y_3Al_6(BO_3)^3Si_6O_{18}(OH)_4$ where X = Na and/or Ca and Y = Mg, Li, Al, and/or Fe2+)

  B, Rb-Sr ρ= 3.0-3.3

Panned Gold

Metal Au **(Ag, S, Pb)** **Density** 19.32

Augé et al, 2015

Minerals inside boulders or glacial sandstone erratics

Figure 4. Different boulder types. a) Carbonate rock. b) Amygdaloidal metabasalt. c) Quartzite. d) Sulfide-bearing mica schist. e) Sandstone. f) Weakly mineralized sandstone. Hammer head and handle lengths 14 and 60 cm, respectively.

Mineral	Formula	Density
Chalcopyrite	**CuFeS2 (Pb)**	4.1–4.3
Pyrite	**FeS**2	5–5.02
Galena	**Pb**S	7.2–7.6
Sphalerite	**(Zn,Fe)S**	3.9–4.2
Pyrrhotite	**Fe**(1-x)S	4.58–4.65
Scheelite	$CaWO_4$ **(Sr-Pb)**	5.3

Hanski et al, BGSF, 2019

Mass spectrometers with ICP ionization source ICP-MS

Teledyne
Solid State 193
nm laser

Autosampler

Desolvating
Nebulizer

Nu instruments
ICP (SC and MC) MS

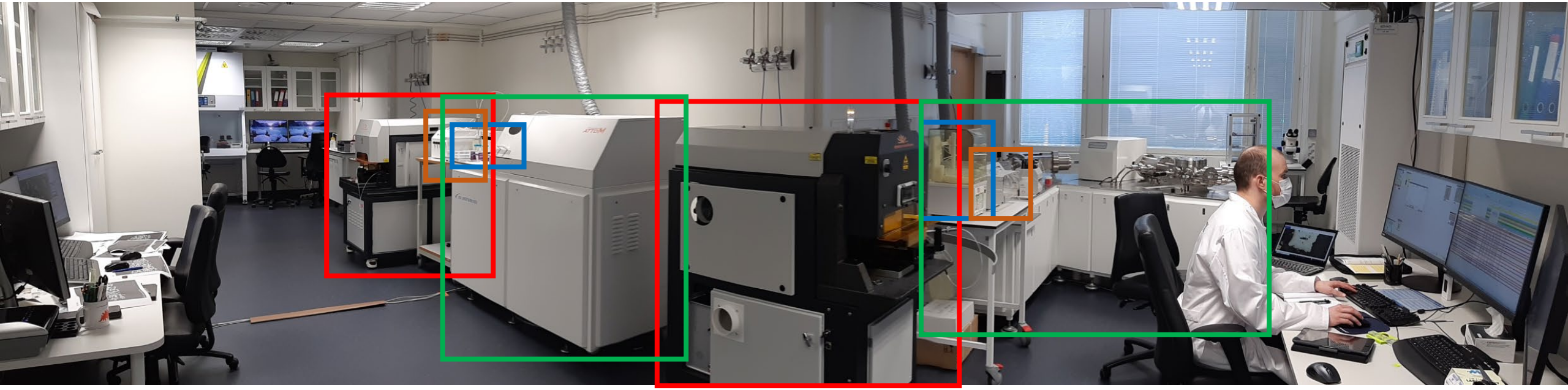

- High ionisation potential
- Design for isotope measurments
- Versatile samples (liquids and solids)
- High dynamic range (from major elements to ultra traces)
- High sample output

Single Collector HR ICP-MS

Multiple Collector HR ICP-MS

Both instruments can be connected to a laser ablation system

Clean chemistry laboratories

Low precision isotope ratio:

- ***Trace element geochemistry***

Liquid (ppq limit of detection)
Solid (any material)

- ***U-Pb geochronology***

(zircon, monazite, baddeleyite, titanite, apatite, xenotime, uraninite…)

High precision isotope ratio on single elements:

- ***Solution analysis (water or dissolved materials)***

Li, Mg, S, Cu, Fe, Zn, Rb, Sr, Sm, Nd, Hf, Th, Pb, U

- ***Minerals:*** Sulfides (S, Fe, Cu, Zn), tourmaline (B) Plagioclase-carbonate (Sr), monazite (Nd), zircon (Hf) Pb (Pb-rich phases)…

Preparation:
In situ isotopic compositon of minerals by laser ablation- ICP (MC MS)

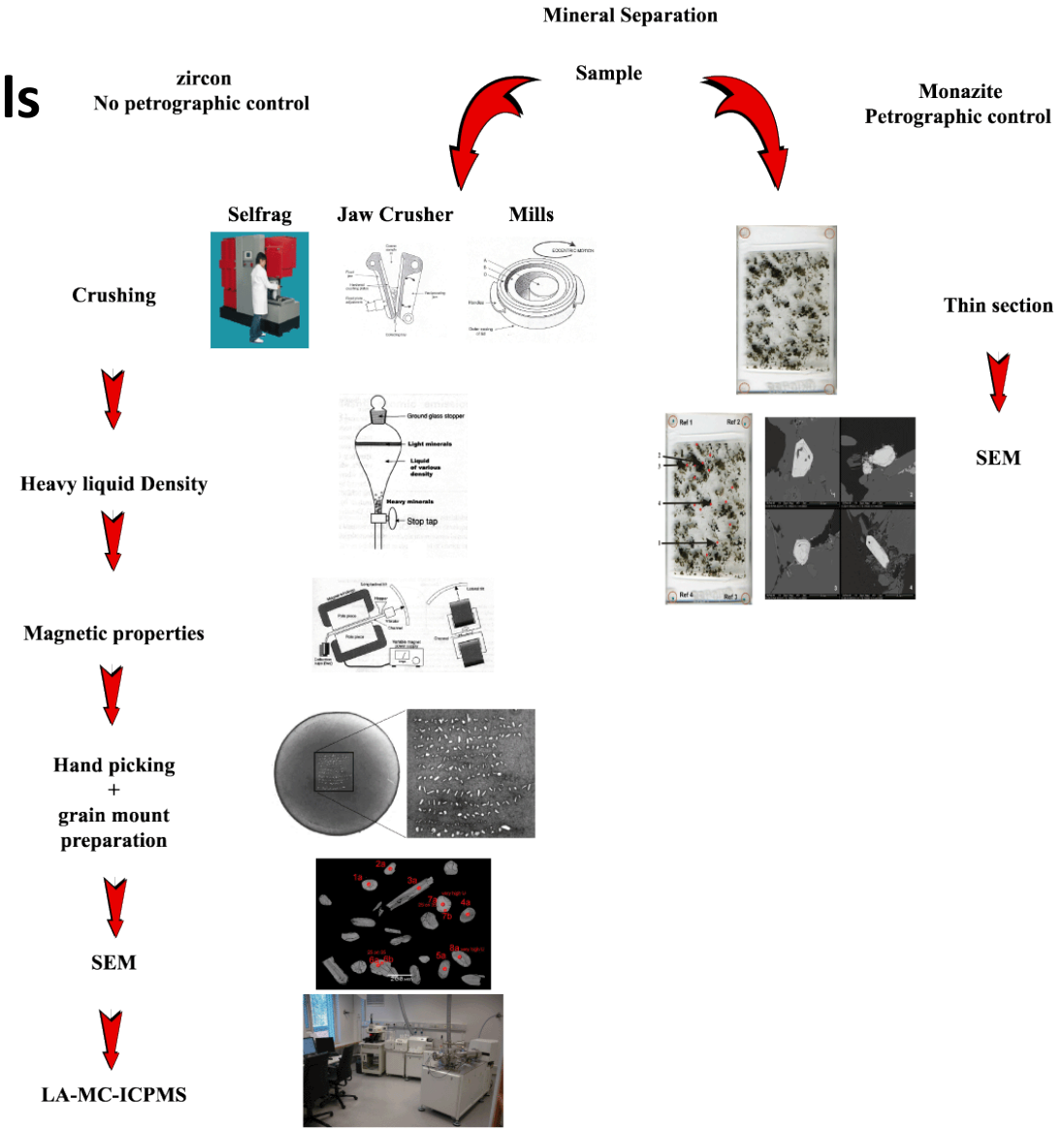

The combined use of SEM and LA (MC) ICP-MS

The real strength is to link our instruments together, allowing in situ analyses (trace element and isotopic) of minerals of interest

A  B 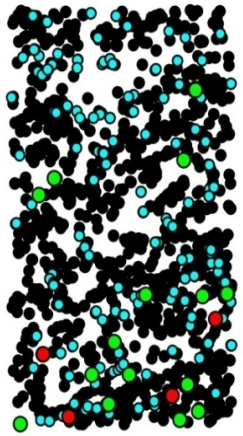

Mineral	Grains	Isotope system
Galena	5	Pb
Monazite	20	U-Pb, Nd
Sulfides	1200	S, Cu
Plagioclase or Diopside	300	Sr

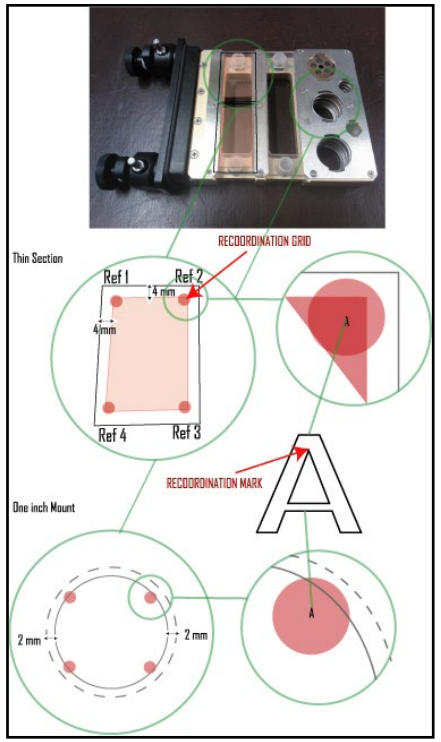

Target grains on a thin section are mapped with the SEM using rapid mineral identification software, coordinates are transferred to laser system.

Direct analysis of grains in situ allows textural information to be retained.

Preparation: Microsampling : Drilling or milling followed by dissolution and chromatography

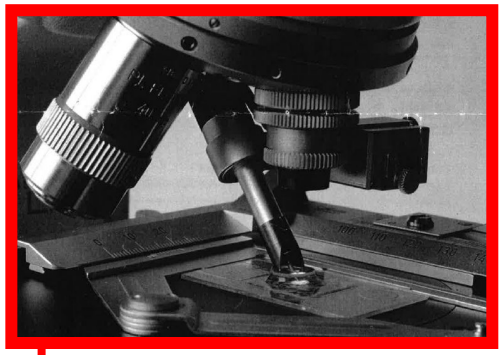

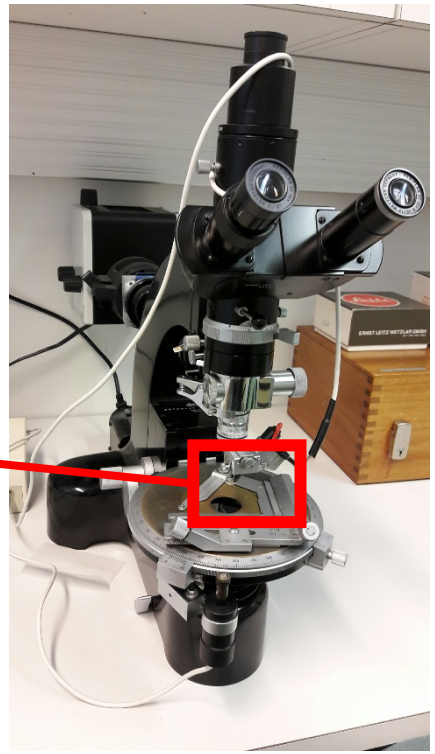

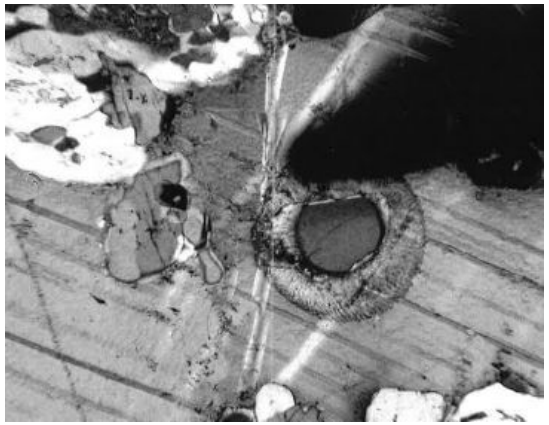

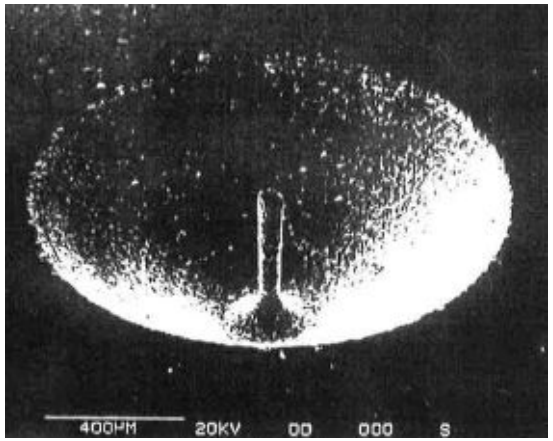

http://www.excitingelectrons.com/microsampling.html
http://www.nwrlasers.com/milling/micromill/

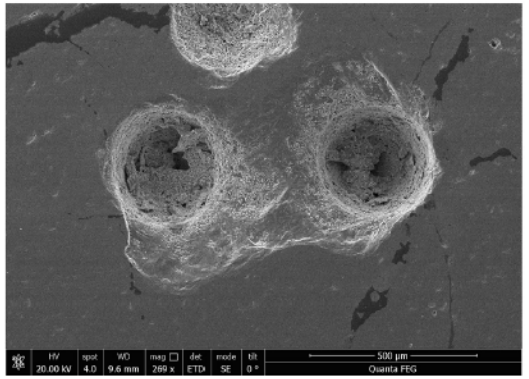

Lv (2020). *IJMS*, **457**,116414.

Preparation: liquid chomatography of dissolved mineral by MC-ICP-MS

Dissolution

Elution

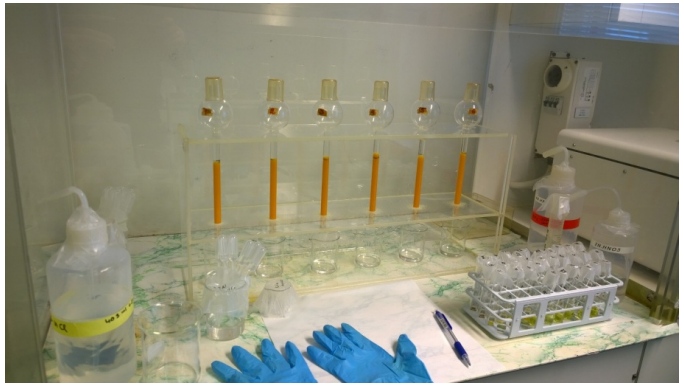

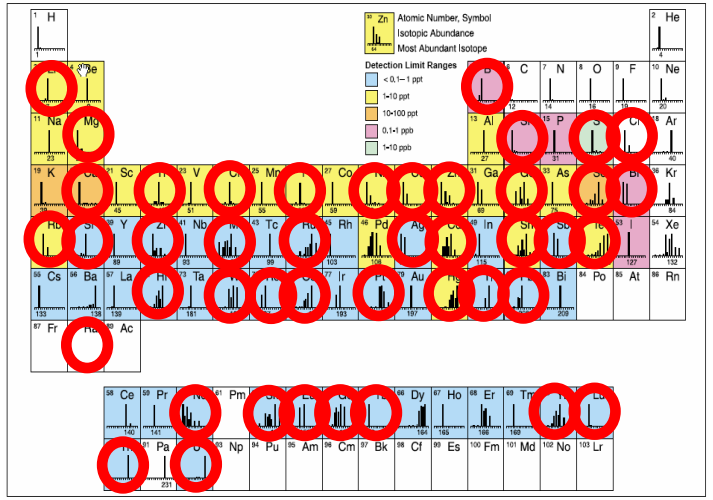

Yang, Mass Spectrometry Reviews, 2009

Dilution

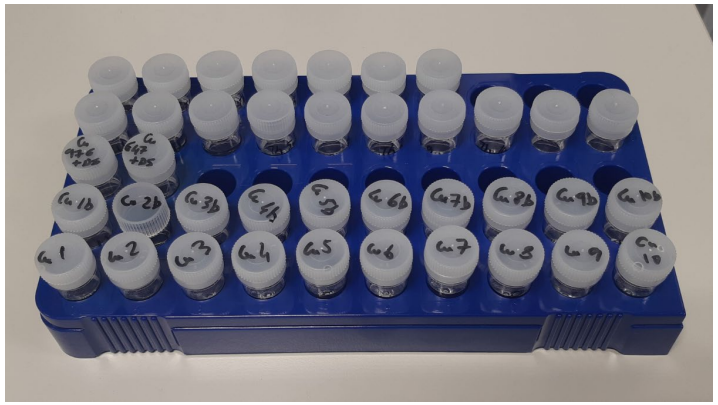

Whole rock analysis on nanopellets

(Garbe-Schönberg, D. & Muller, S, JAAS, 2014)

5cm

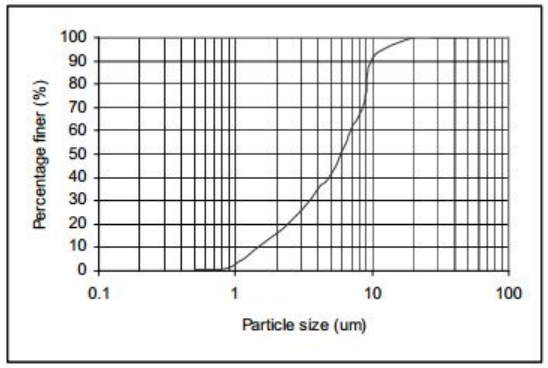

Fig. 1. Particle size distribution characteristics for PFA sample

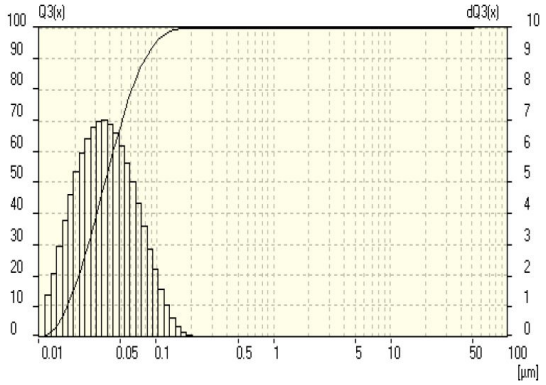

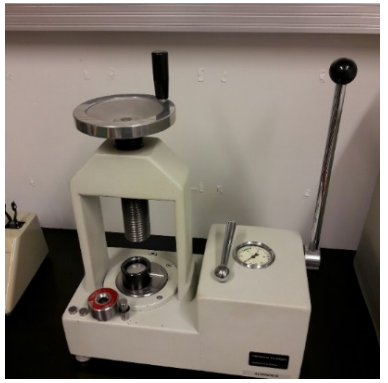

Advantages:

- No melting and dissolution
- Homogeneous standard production

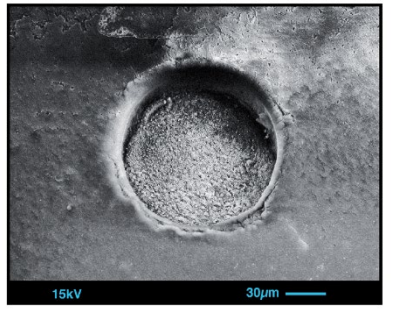

Laser ablation pit in pressed powder pellets

isotope ratio is also used to measure trace element concentrations

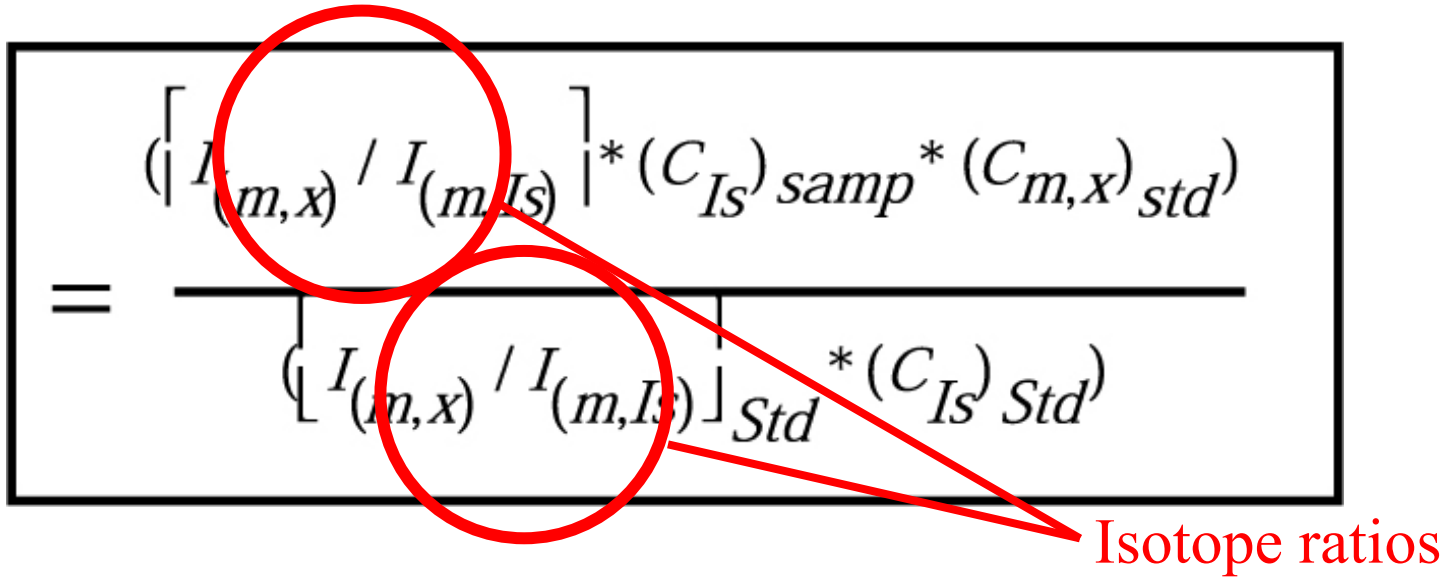

Measuring trace element concentrations is the same as measuring isotope ratios…. But of two different elements

Magnetite

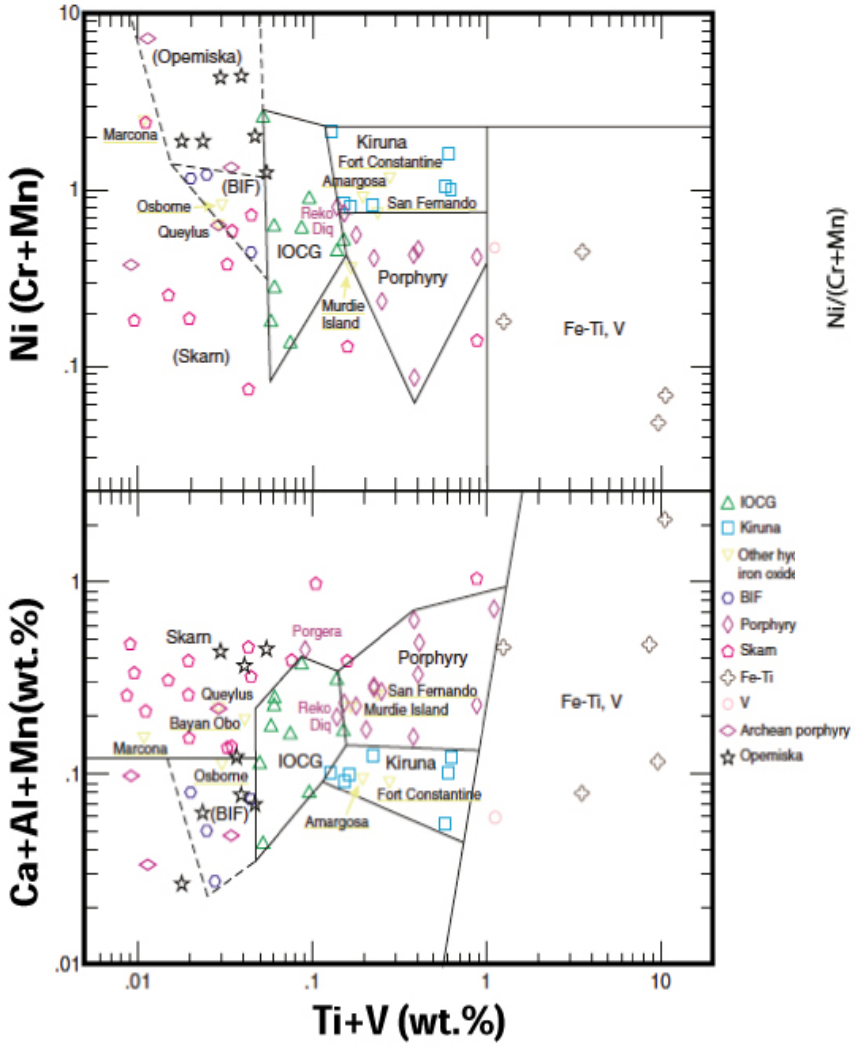

Discriminant diagram for average Fe-oxide compositions from various mineral deposit types. The figure is modified from Dupuis C and Beaudoin G. (2011), Discriminant diagrams for iron iron oxide trace element fingerprinting of mineral deposit types, Mineral deposita, 46: 319-335.

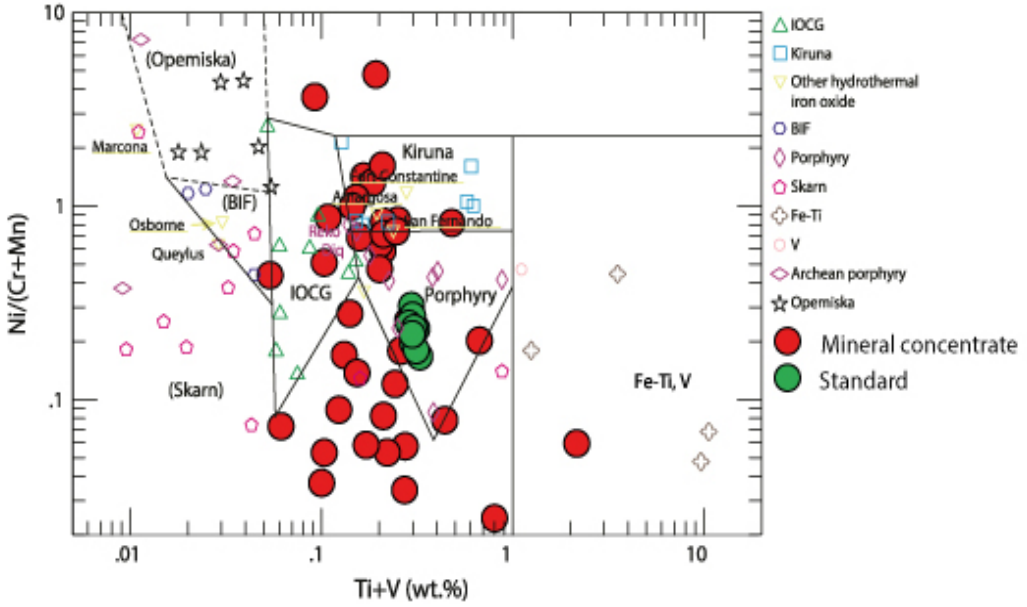

Scheelite (CaWO4)

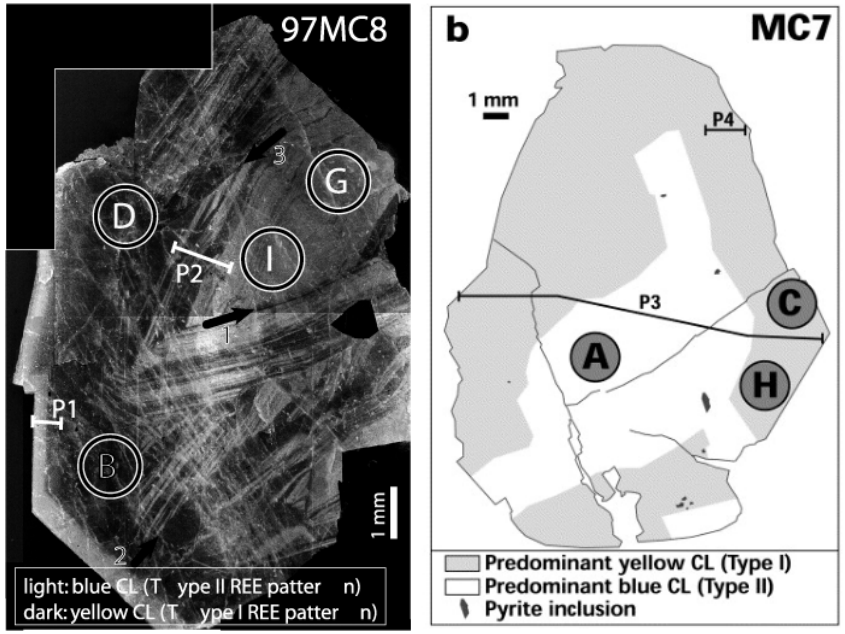

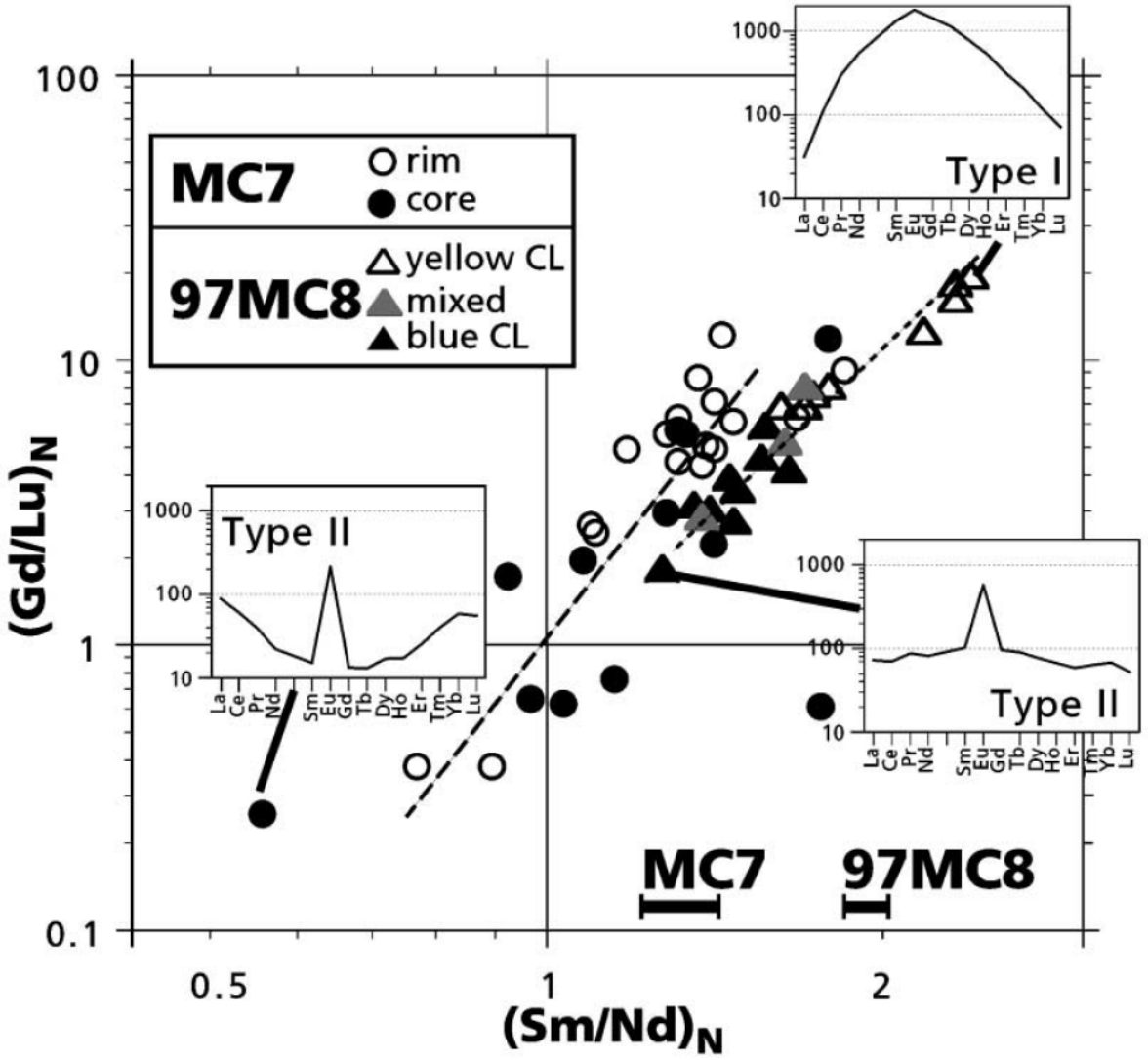

The fractional crystallisation of scheelite from REE-poor hydrothermal solutions leads to the development of a positive Eu-anomaly in scheelite. ***Brugger et al., 2000 Contrib. Mineral.Petrol. 139, 251–264; Brugger et al., 2002 Chem.Geol. 182, 203-225.***

Pyrites : Discrimination between Magmatic or Hydrothermal?

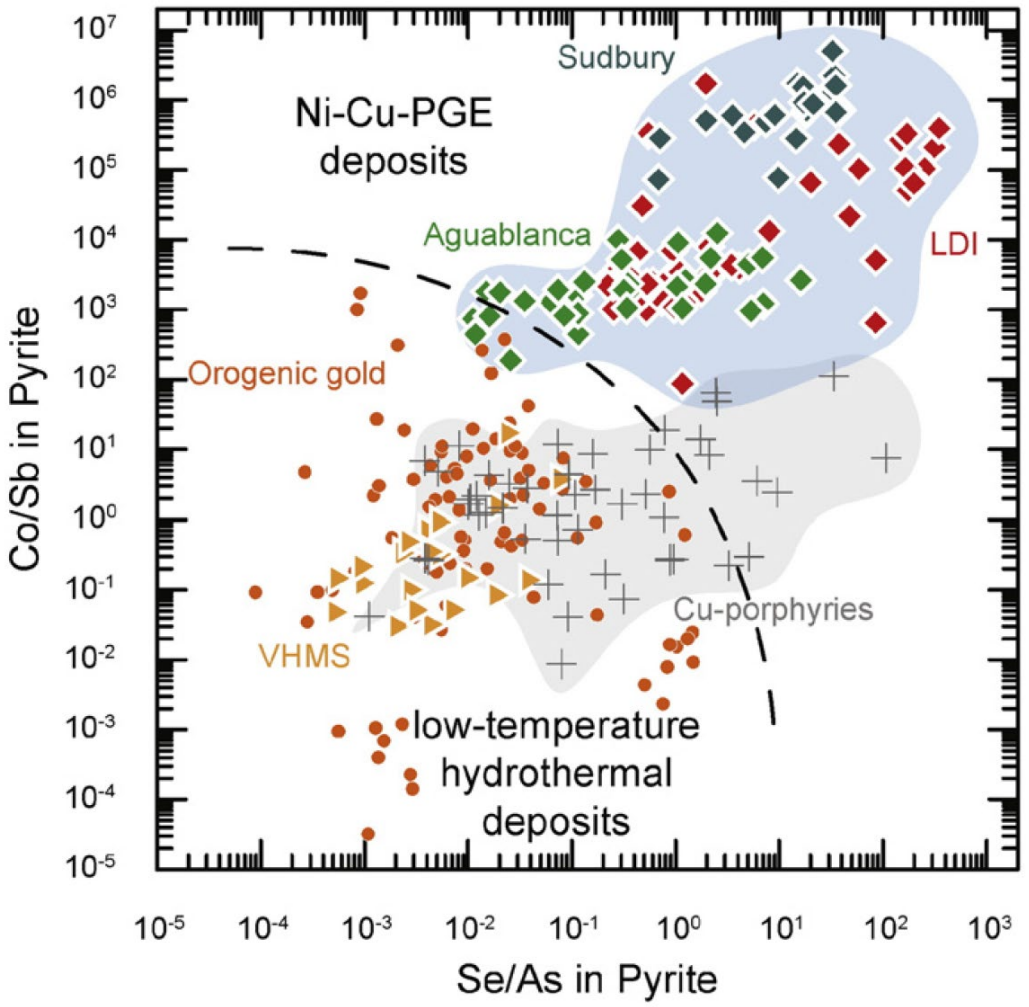

The Co/Sb and Se/As ratios of pyrites from Ni–Cu–PGE deposits strongly differ from pyrites from low-temperature hydrothermal deposits. Therefore, the use of the plot of Co/Sb versus Se/As in pyrite has a strong potential in exploration to discriminate between the possible origins of pyrite in glaciated terrains.

Duran et al., J. Geochem Exploration 2015, 158, 223-242.

Suggested reading for a complete overlook on trace element fingerprinting of minerals

Cook et al., Minerals 2016, 6, 111

Which element for what purpose ?

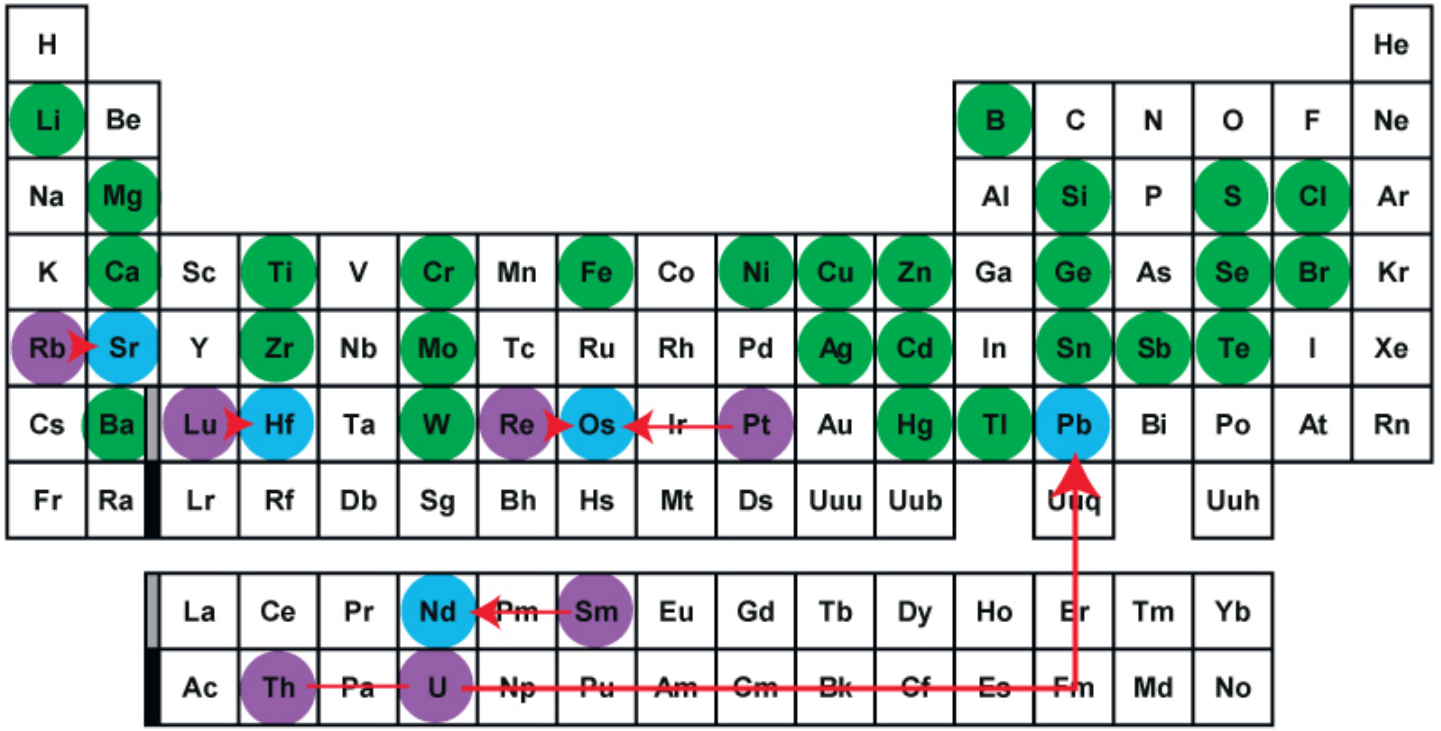

”Useless” elements: mono-isotopic, low ionization, air contamination, very low abundances

Geochronology

Conservative Isotope tracer (information on the source of the metal)

Not always ”conservative” tracers (information on processes: e.g. temperature, redox etc..)

Which element for what purpose ?

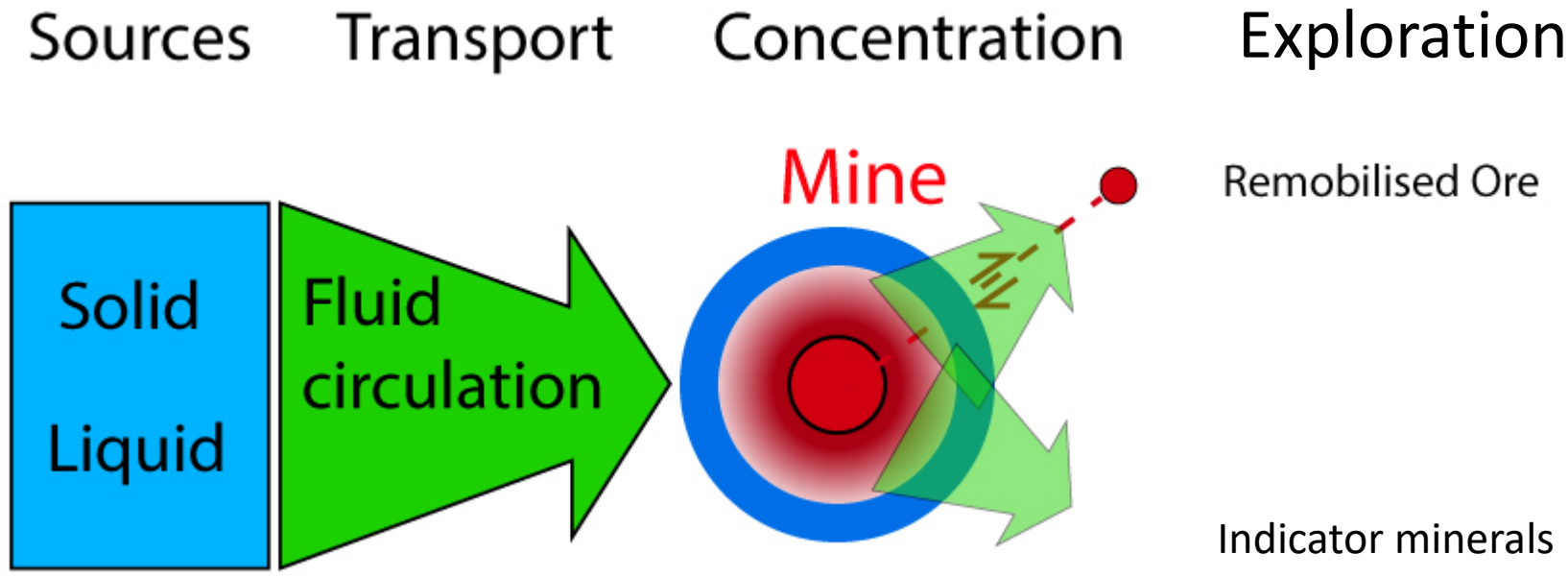

- Radioactive elements: Geochronology (timing of the mineralization (primary and secondary))
- Radiogenic elements: Conservative Isotope tracer (information on the source of the metal)
- Stable elements – not always conservative (information on processes: e.g. temperature, redox etc..)

Which mineral?

Geochronology

Because of unresolved isobaric interferences, only U-Pb on mineral phases trapping U only (not Pb) during crystallisation is possible (zircon, monazites, titanite, rutile, xenotime, urananite…)

Conservative isotopes - Radiogenic isotopes

- The concentration in the sample has to be high enough
- Only a limited abundance of interferences can be corrected (no chemical separation)

Problem for β-decay systems: Parent- and daughter isotopes have the same mass

(e.g. $^{87}Rb \rightarrow {}^{87}Sr$ (plagioclase); $^{176}Lu \rightarrow {}^{176}Hf$ (zircon), $^{187}Re \rightarrow {}^{187}Os$ (sulphides), $^{147}Sm \rightarrow {}^{143}Nd$ (monazite)

➔ no isochron dating possible for those systems

only model ages and tracer studies

Not always conservative isotope- Stable isotopes

- Sulphides (S, Cu, Fe, Zn)
- Oxides (Fe)
- Silicates: Tourmaline (B), spodumene (Li)

Geochronology

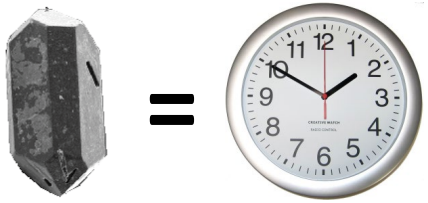

$^{235}U \rightarrow {}^{207}Pb$ t ½ = 0.704 Ga

$^{238}U \rightarrow {}^{206}Pb$ t ½ = 4.468 Ga

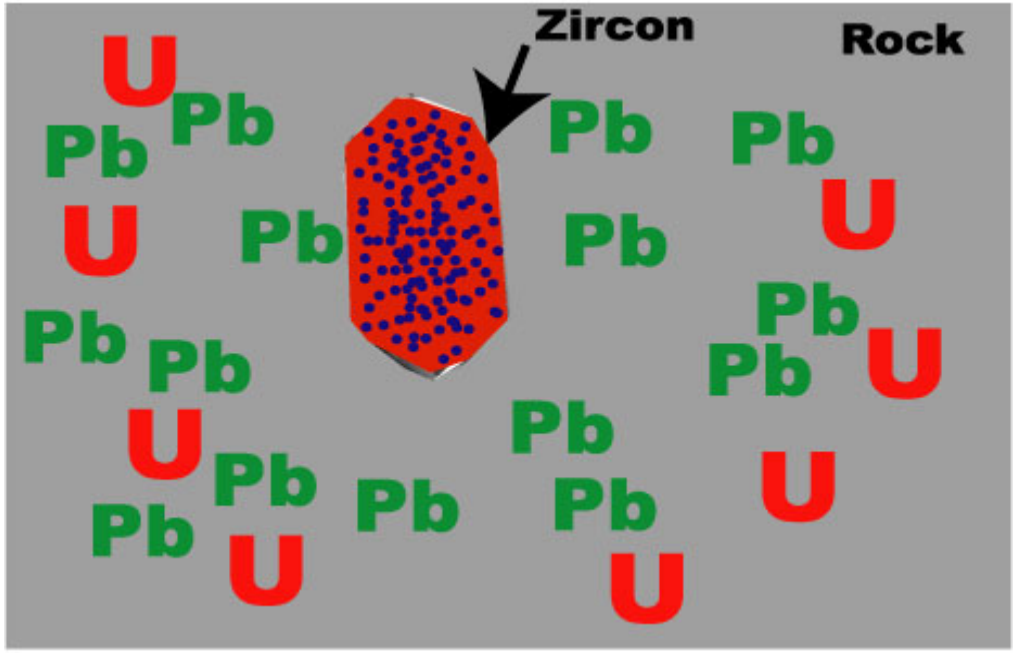

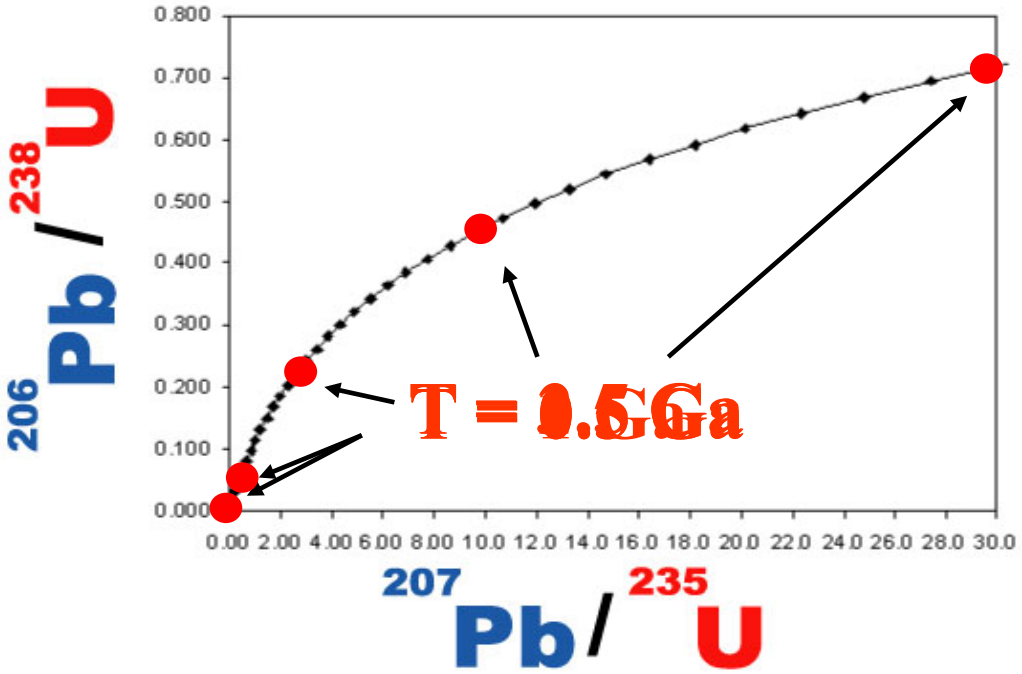

Pb = Common Lead

Pb = Radiogenic Lead

Zircon - $ZrSiO_4$

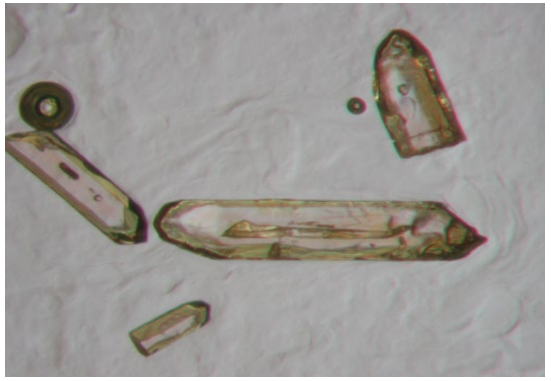

Baddeleyite - ZrO_2

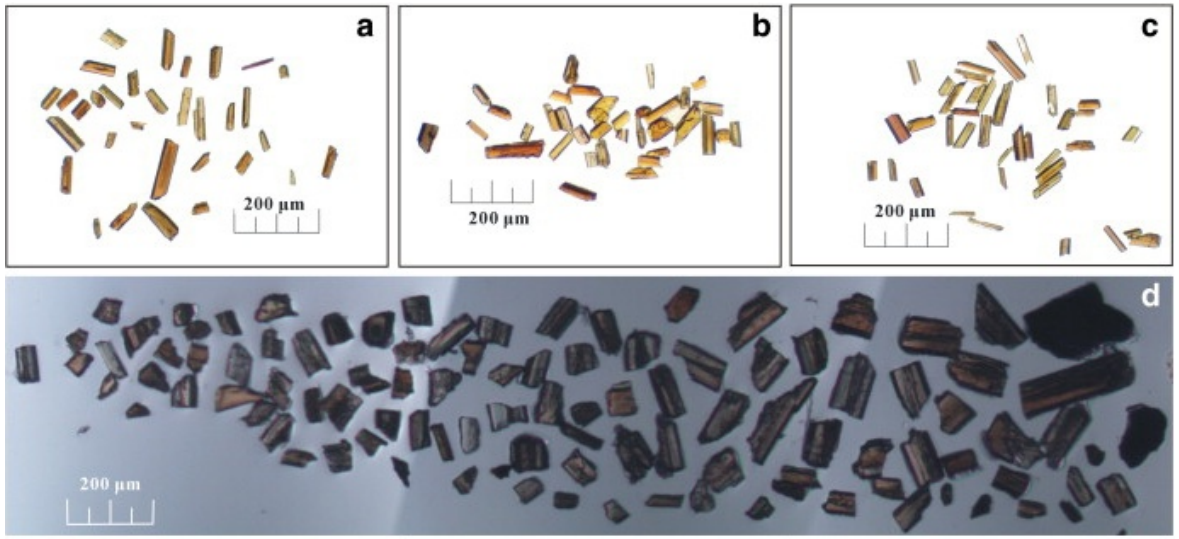

Monazite - $(Ce,La,Th)PO_4$

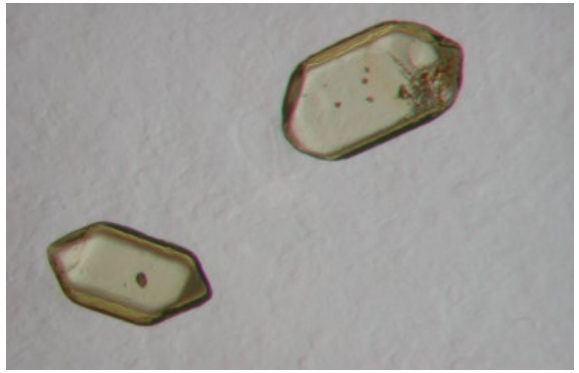

Xenotime – YPO_4

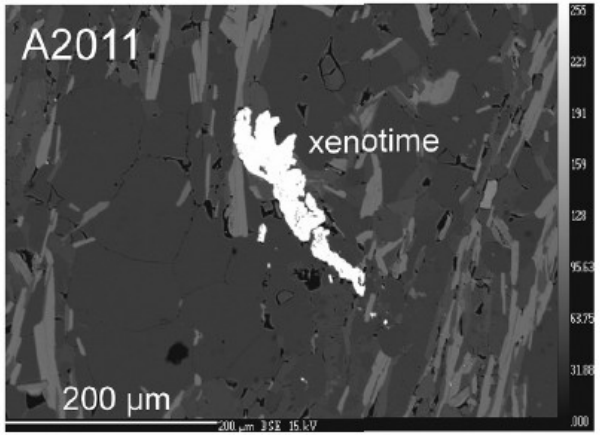

Titanite / Sphene – $CaTiSiO_5$

Rutile- TiO_2

Apatite, Perovskite, Urananite, Carbonate, Cassiterite, Wollastonite, Garnet……

Lead

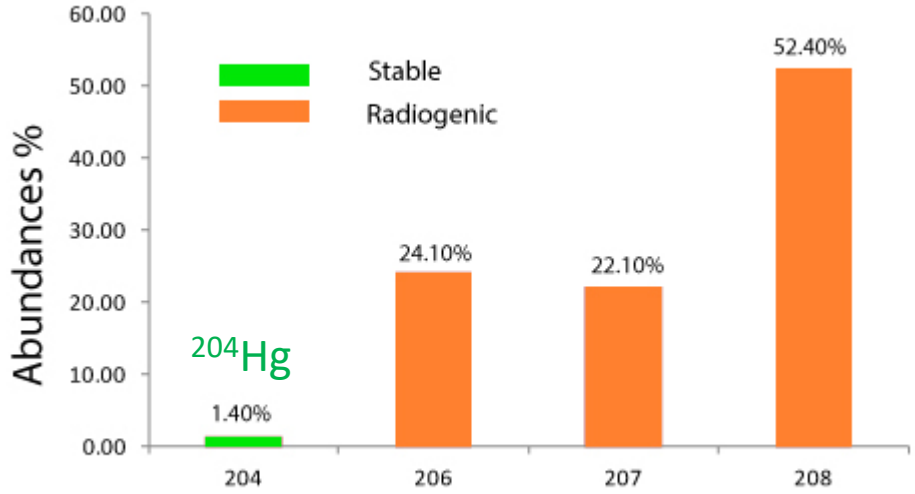

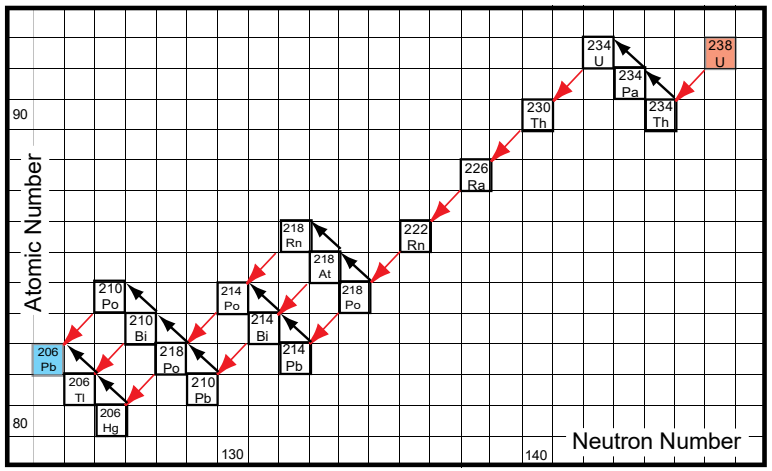

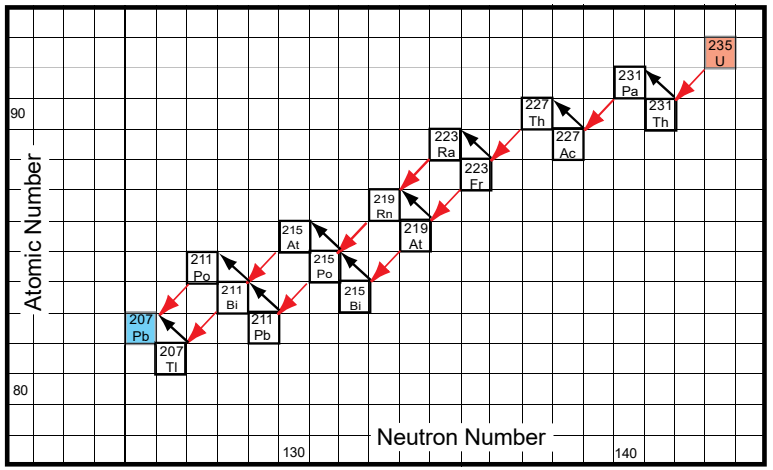

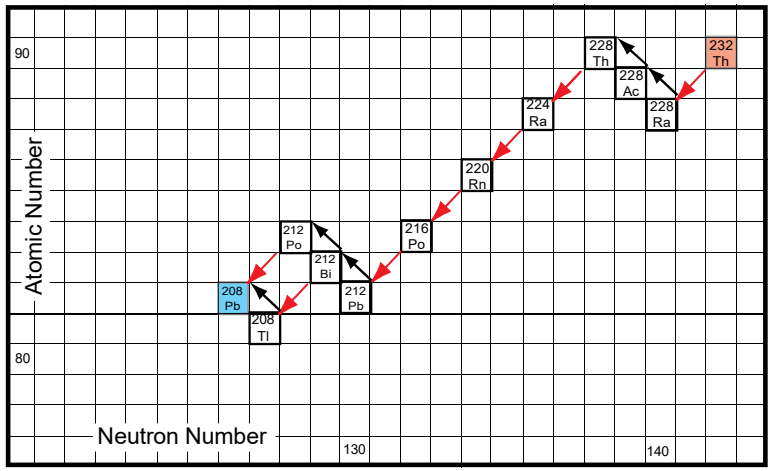

Parent	Decay Mode	λ	Half-life	Daughter	Ratio
^{232}Th	α,β	$4.948 \times 10^{-11} y^{-1}$	$1.4 \times 10^{10} y$	^{208}Pb, 8 ^{4}He	$^{208}Pb/^{204}Pb$, $^{3}He/^{4}He$
^{235}U	α,β	$9.849 \times 10^{-10} y^{-1}$	$7.07 \times 10^{8} y$	^{207}Pb, 7 ^{4}He	$^{207}Pb/^{204}Pb$, $^{3}He/^{4}He$
^{238}U	α,β	$1.551 \times 10^{-10} y^{-1}$	$4.47 \times 10^{9} y$	^{206}Pb, 6 ^{4}He	$^{206}Pb/^{204}Pb$, $^{3}He/^{4}He$

Mineralisation model age dating based on Galena Pb-Pb

Haopinggou Au-Ag-Pb-Zn deposit, SE China craton,
the most important Mo, Au, Ag resource province in China

Gold minerals are enriched in Stage 1
pyrite-quartz veins

Silver minerals are enriched in Stage 2
Pb-Zn-sulfide veins

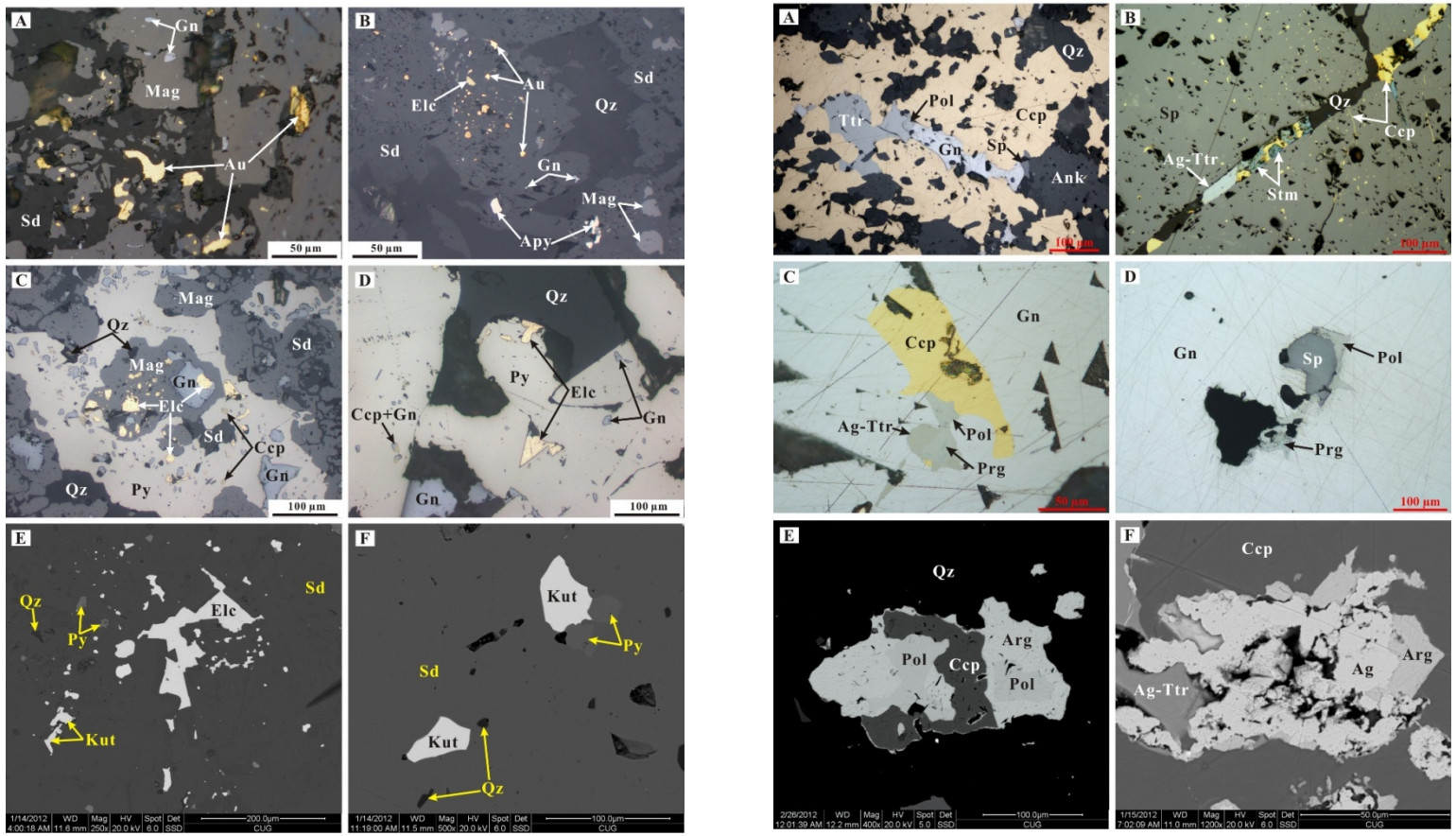

Li Z-K et al (2016)
Textures, trace elements, and Pb isotopes of sulfides from the Haopinggou vein deposit, southern North China Craton: implications for discrete Au and Ag-Pb-Zn mineralization. *Contributions to Mineralogy and Petrology*, **171**,99.

Mineral Exploration Targeting

eit RawMaterials Connecting matters

Funded by the European Union

eit RawMaterials ACADEMY

Minearlisation model age dating based on Galena Pb-Pb

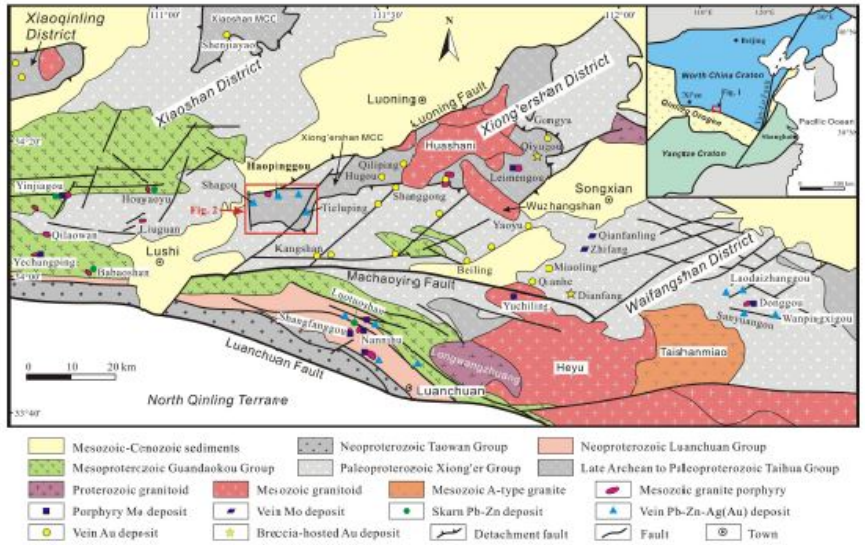

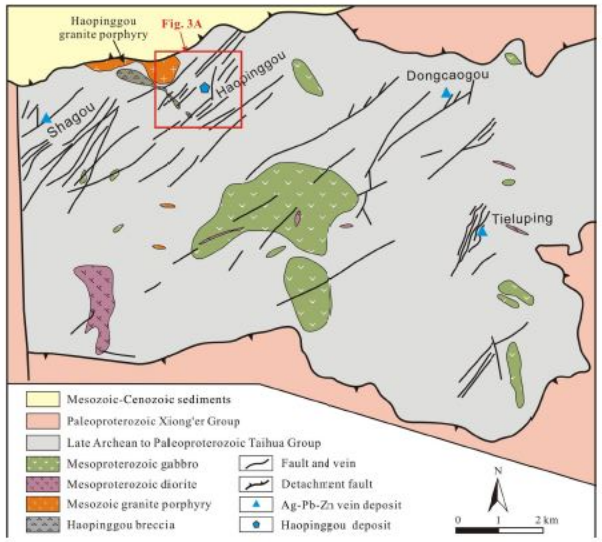

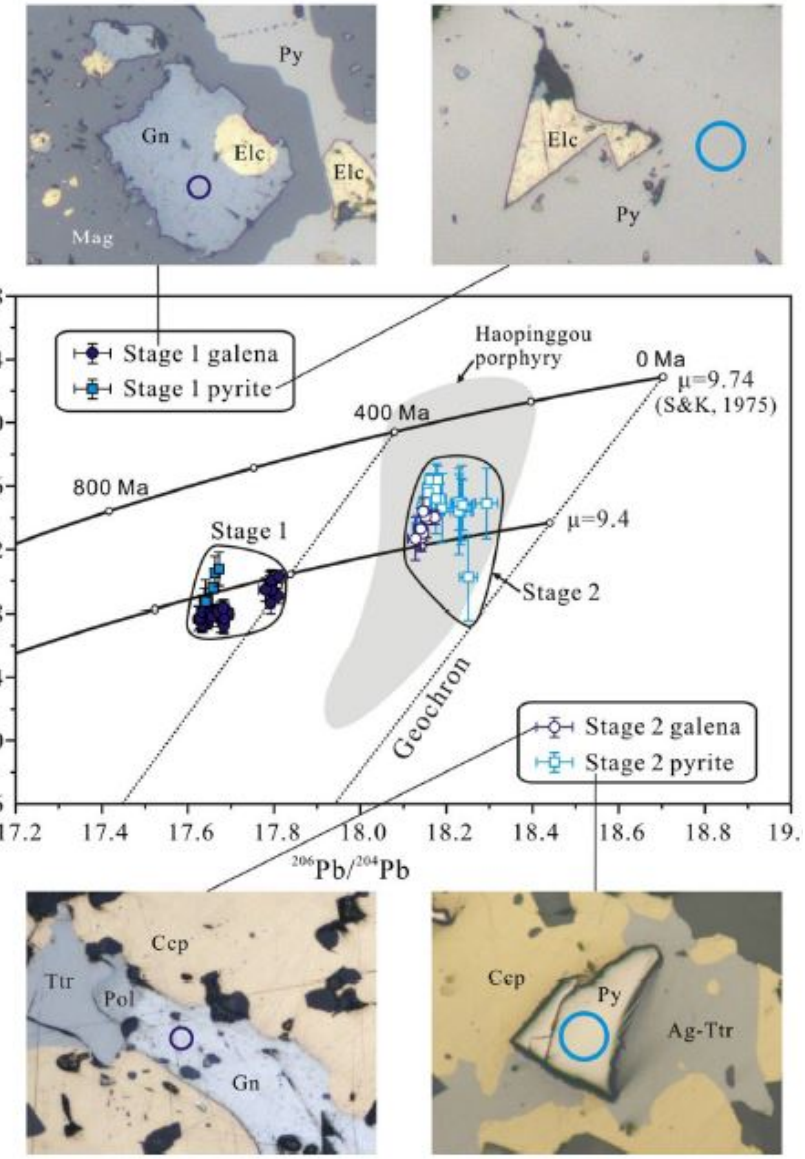

Li Z-K et al (2016)
Textures, trace elements, and Pb isotopes of sulfides from the Haopinggou vein deposit, southern North China Craton: implications for discrete Au and Ag-Pb-Zn mineralization. *Contributions to Mineralogy and Petrology*, **171**,99.

Pb isotopes from Finnish Zn-Pb-Cu sulfide-bearing boulders

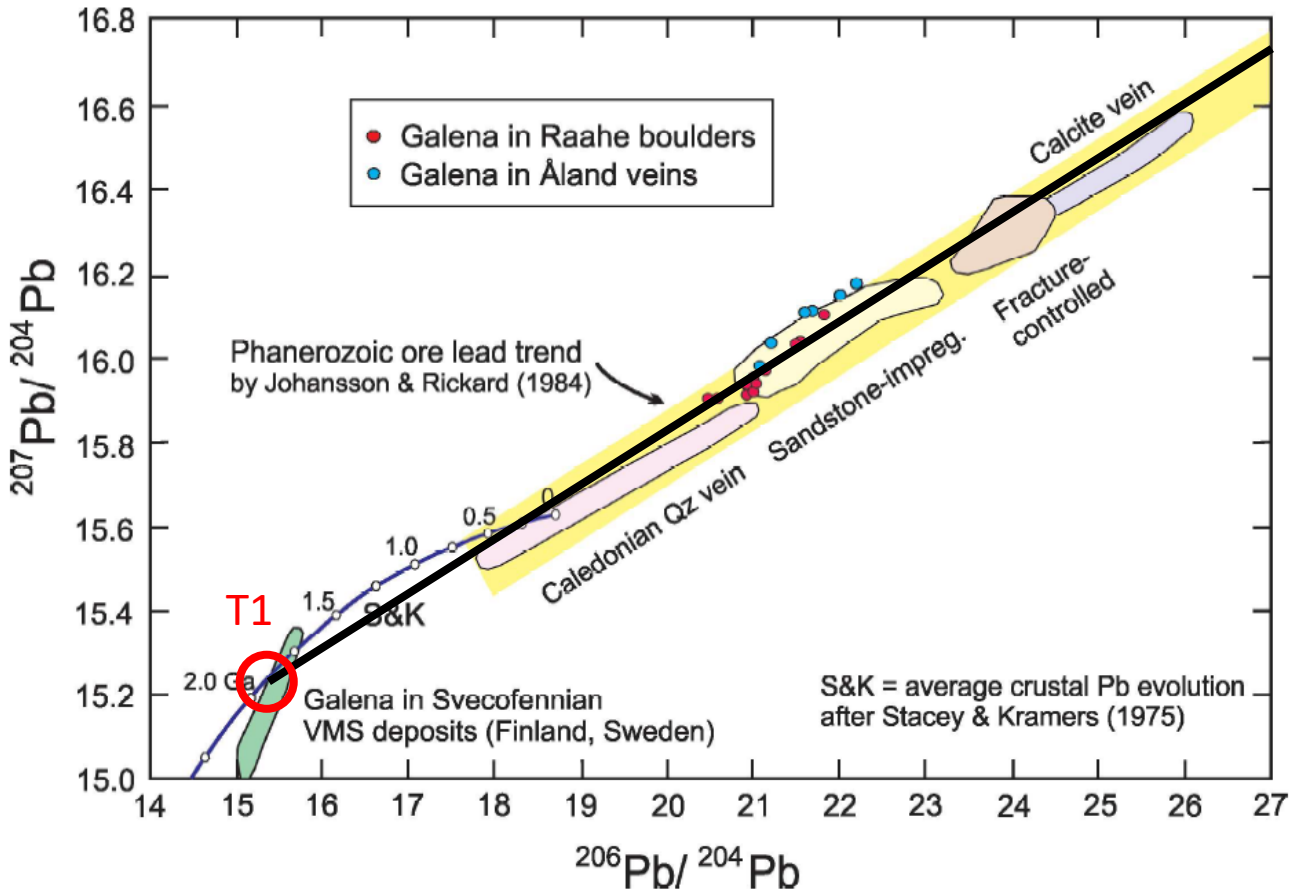

$$slope = \frac{1}{137.88} * \frac{(e^{\lambda 235\, T1} - (e^{\lambda 235\, T2})}{(e^{\lambda 238\, T1} - (e^{\lambda 238\, T2})}$$

T1 = 1.9Ga

T2 = Caledonian 450-500Ma

Hanski et al (2019) *Bulletin of the Geological Society of Finland*, **91**,143-178

Combining geochronological information from several heavy minerals

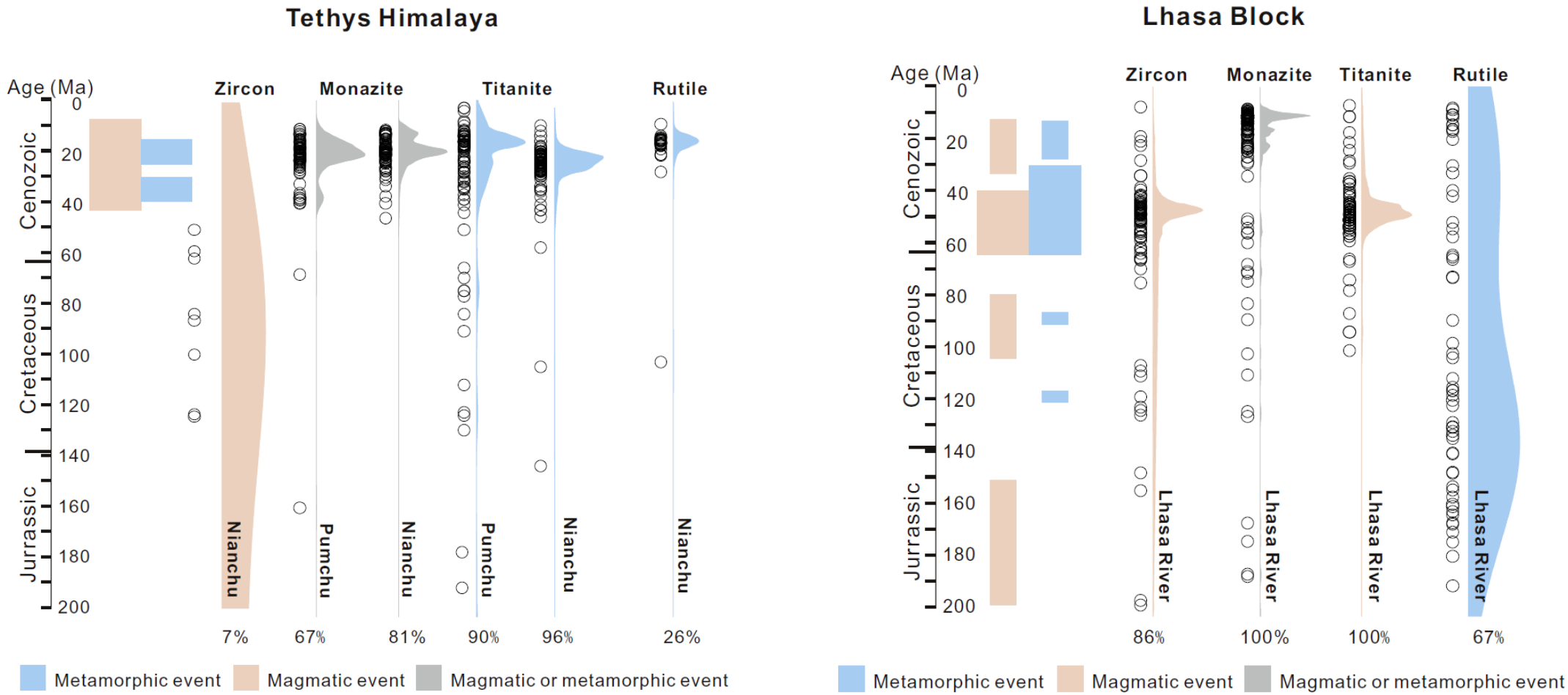

Guo R, Hu X, Garzanti E, Lai W, Yan B & Mark C (2020) How faithfully do the geochronological and geochemical signatures of detrital zircon, titanite, rutile and monazite record magmatic and metamorphic events? A case study from the Himalaya and Tibet. *Earth-Science Reviews*, **201**,103082

Combining information from trace elements and isotopic ratio on heavy mineral apatite

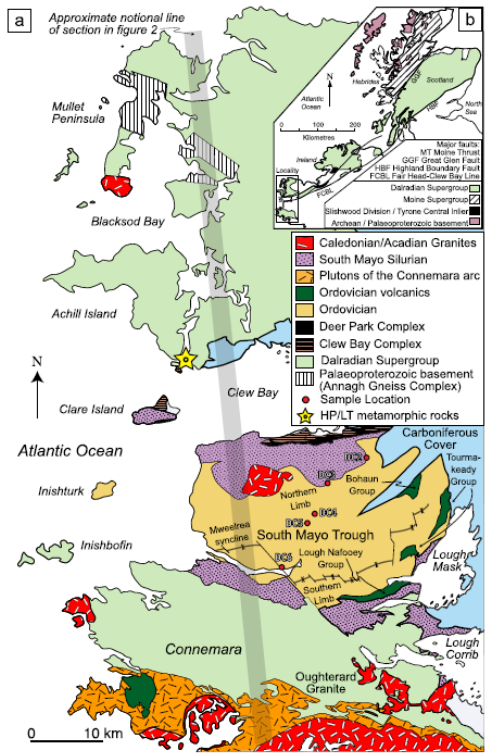

Fig. 1. Location (inset) and geological map of the South Mayo Trough and relevant surrounding areas, modified from Chew et al. (2007).

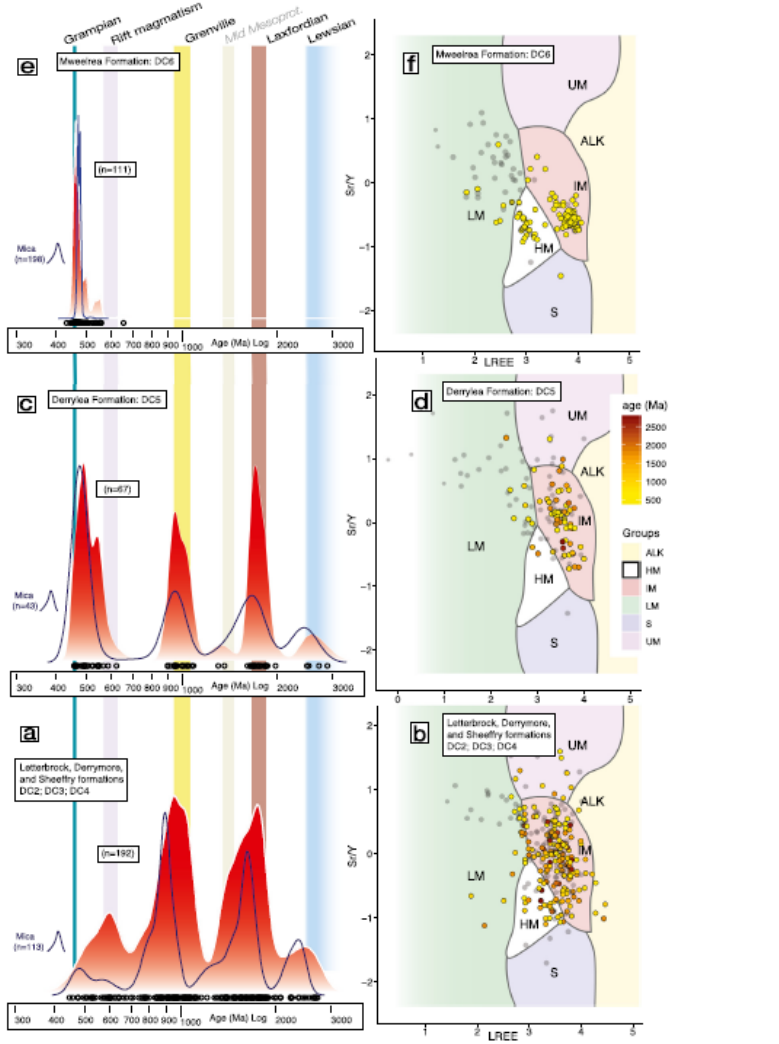

Fig. 4. Kernel density plots and support vector machine (SVM) apatite classification diagrams (Sr/Y vs LREE [La, Ce, Pr, Nd]) for South Mayo Trough apatite detritus. The category acronyms on SVM biplots are ALK — alkaline-rich igneous; HM — high-grade metamorphic; IM — I-type granitoids and mafic igneous; LM — low- and medium-grade metamorphic; S — S-type granites; UM — ultramafic igneous. Grains that provide no ages are coloured grey on SVM biplots.

O'Sullivan GJ & Chew DM (2020) The clastic record of a Wilson Cycle: Evidence from detrital apatite petrochronology of the Grampian-Taconic fore-arc. *Earth and Planetary Science Letters*, **552**,116588.

Mao M, Rukhlov AS, Rowins SM, Spence J & Coogan LA (2016) Apatite Trace Element Compositions: A Robust New Tool for Mineral Exploration. *Economic Geology*, **111**,1187-1222.

Radiogenic isotopes – Isotopic fingerprinting

Which isotope systems are suitable for isotopic fingerprinting by laser ablation ?

- The concentration in the sample has to be high enough

- Only a limited abundance of interferences can be corrected (no chemical separation)

Problem for β-decay systems: Parent- and daughter isotope have the same mass (e.g. $^{87}Rb \rightarrow {}^{87}Sr$; $^{176}Lu \rightarrow {}^{176}Hf$)

➔ no isochron dating possible for those systems
only model ages and tracer studies (Hf, Sr, Os, Nd)

Conservative isotopes - Radiogenic isotopes

$$\frac{^{176}Hf}{^{177}Hf} = \left(\frac{^{176}Hf}{^{177}Hf}\right)_0$$

Zircon, Eudialyte

$$\frac{^{143}Nd}{^{144}Nd} = \left(\frac{^{143}Nd}{^{144}Nd}\right)_0$$

Monazite, loparite, apatite

$$\frac{^{87}Sr}{^{86}Sr} = \left(\frac{^{87}Sr}{^{86}Sr}\right)_0$$

Plagioclase, Clinopyroxene, carbonate, apatite…

$$\frac{^{187}Os}{^{188}Os} = \left(\frac{^{187}Os}{^{188}Os}\right)_0$$

Sulfides (Laurite in chromite)

Example: Rb-Sr system

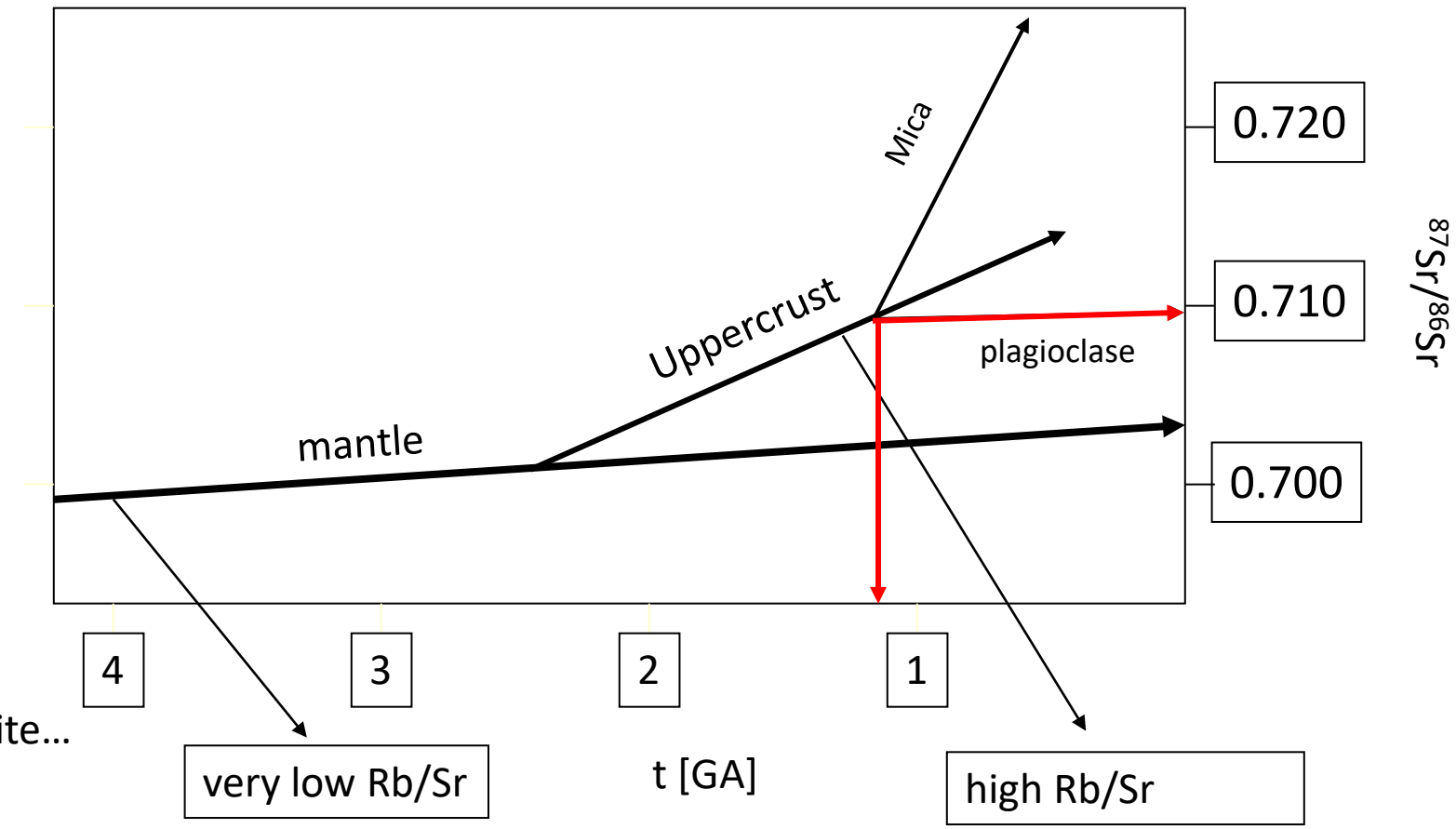

Unchanged isotopic composition

Model age calculation possible

Applications: Crustal contamination and mineralisation

Example from the Bushveld complex (SA)

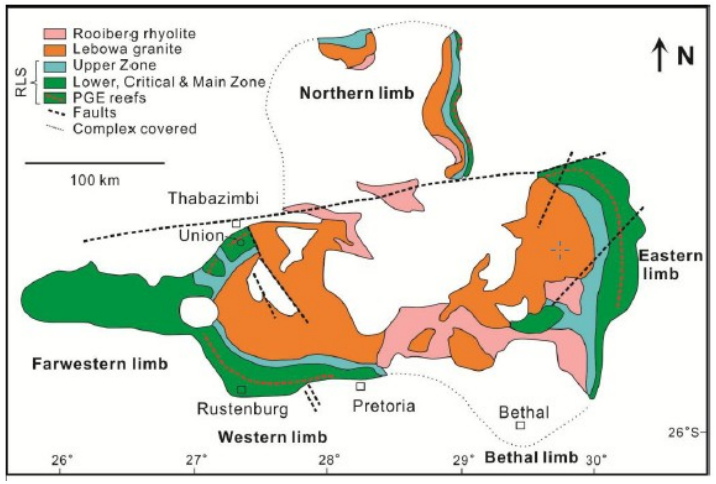

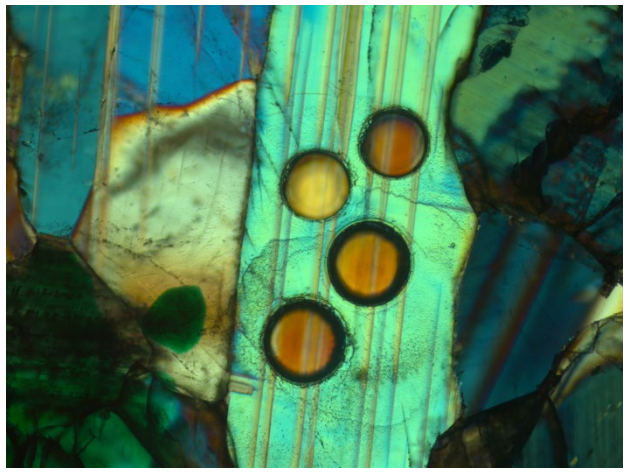

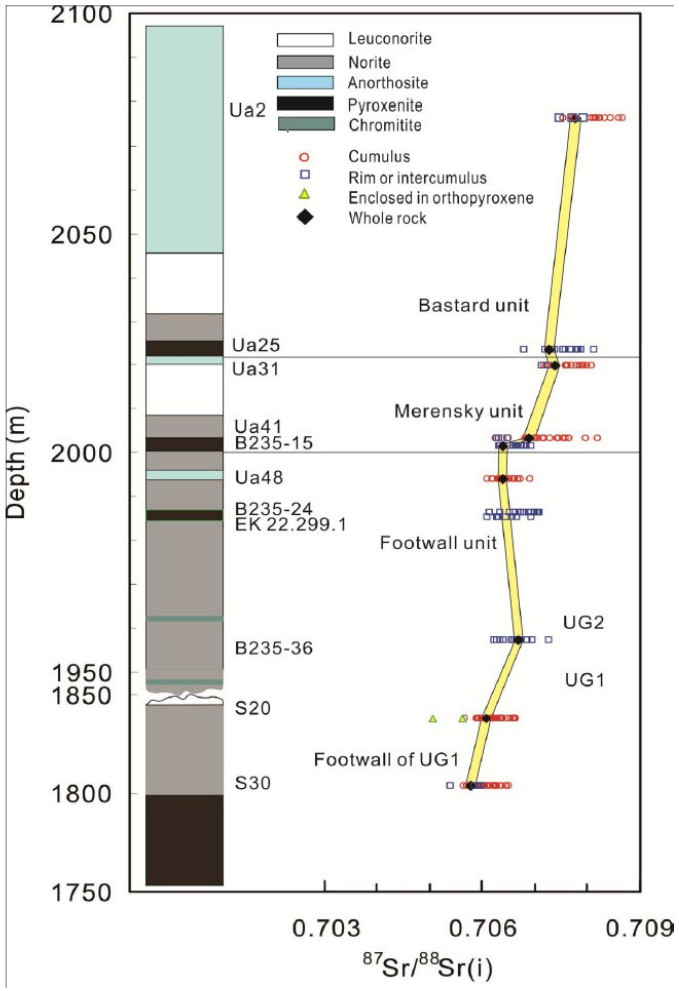

and from the Kevitsa intrusion (Finland)

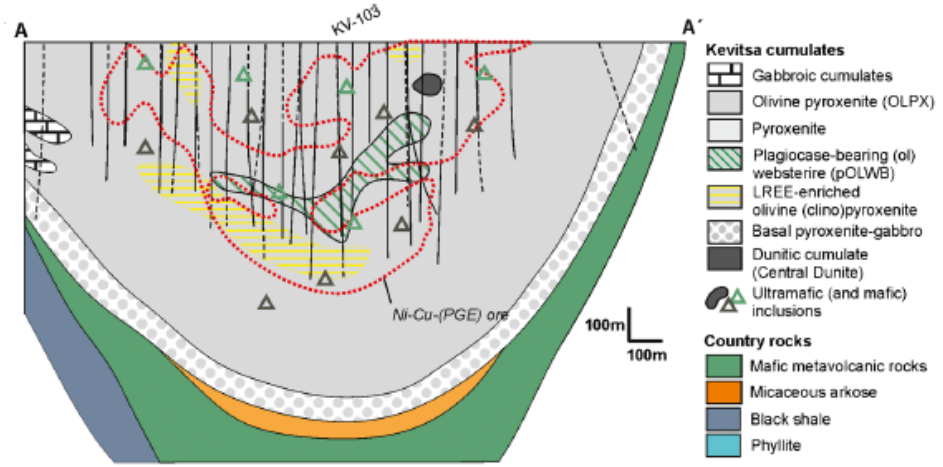

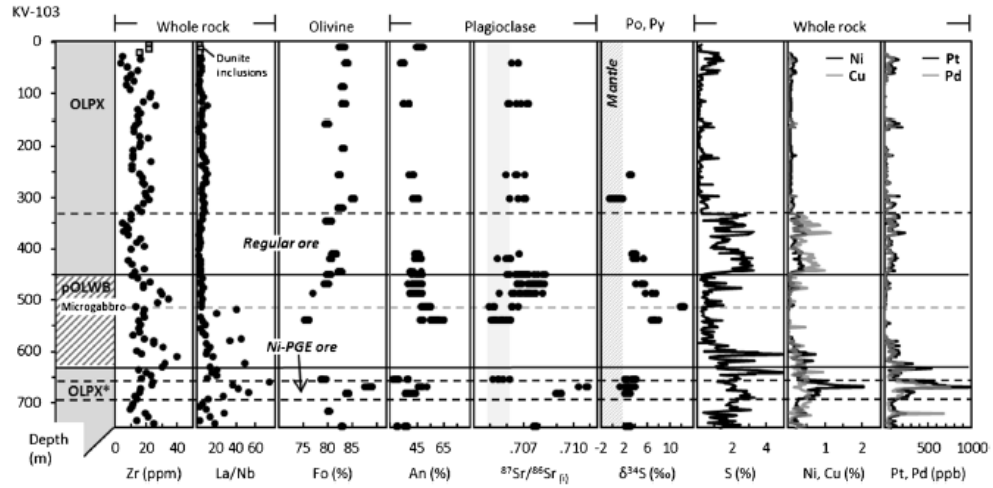

Yang et al, 2013

Radiogenic isotopes – Isotopic fingerprinting : Sm-Nd on monazite

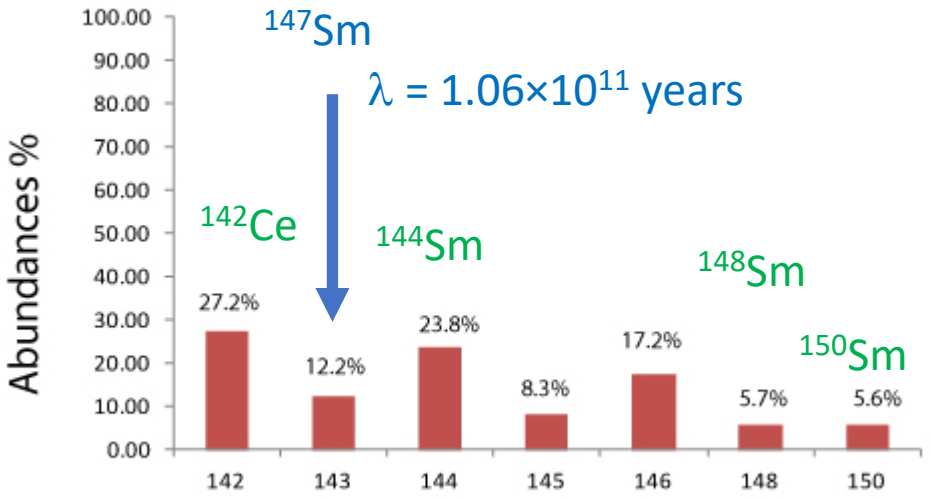

$^{143}Nd/^{144}Nd$ as a function of the protolith age

$^{146}Nd/^{144}Nd$=0.7219
Natural ratio for mass bias correction

Sensitivity and spatial resolution limitations

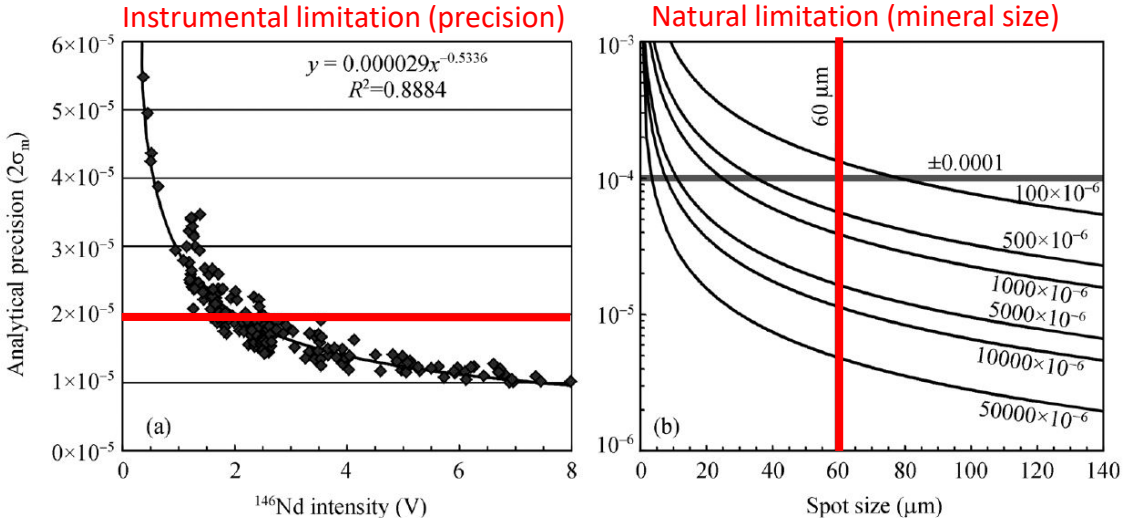

YANG, Y., J. SUN, L. XIE, H. FAN, and F. WU, 2008.
In situ Nd isotopic measurement of natural geological materials by LA-MC-ICPMS. Chinese Science Bulletin 53: 1062-1070.

Application to detrital monazites

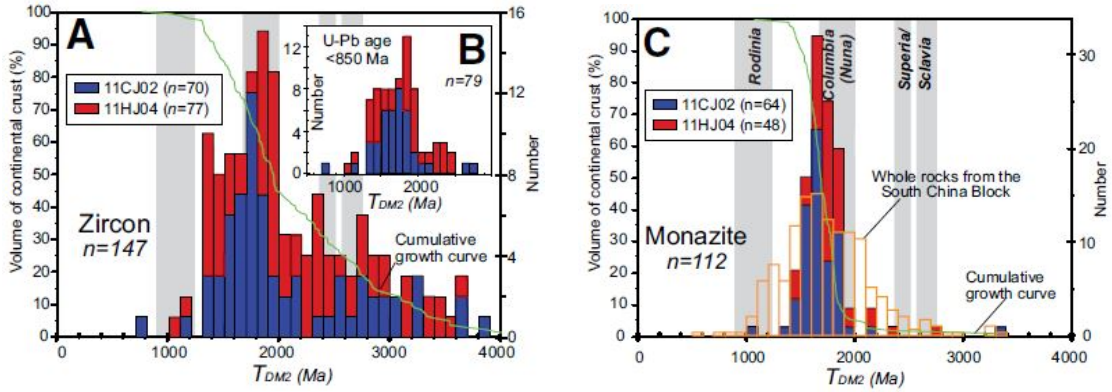

Liu et al, 2017.
Tracing crustal evolution by U-Th-Pb, Sm-Nd, and Lu-Hf isotopes in detrital monazite and zircon from modern rivers.
Geology 45: 103-106.

Non-traditional stable isotope tracers of mineralization processes

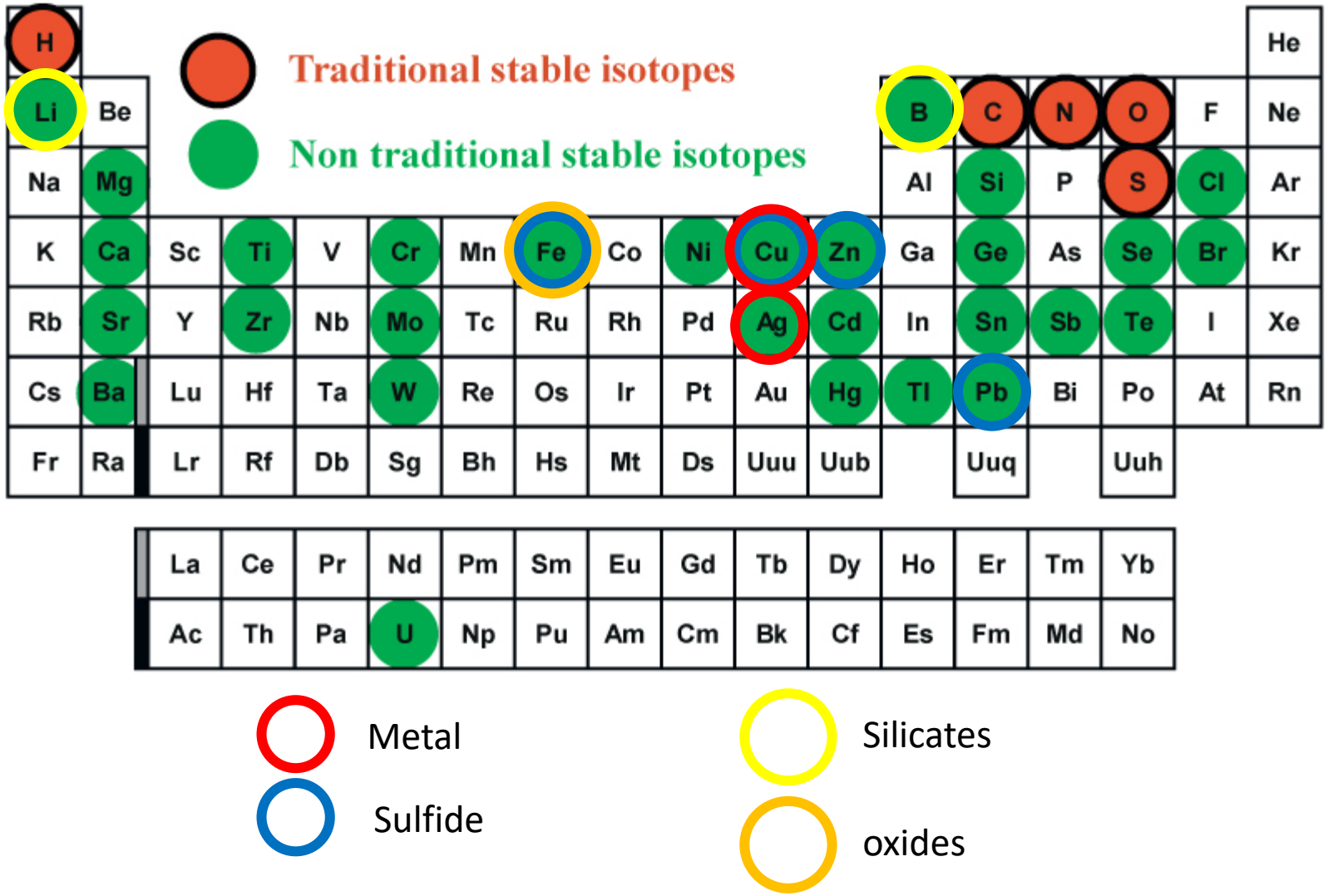

Two main types of stable isotope fractionation

- Non-equilibrium (kinetic) fractionation- unidirectional reactions: Temperature changes, Product removal, Most biological reactions

(**different reaction rates of light and heavy isotopes**)

- Equilibrium fractionation

(reactions proceeding at equal rates)

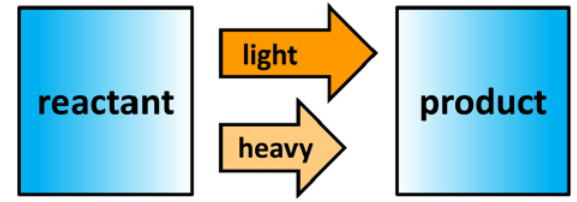

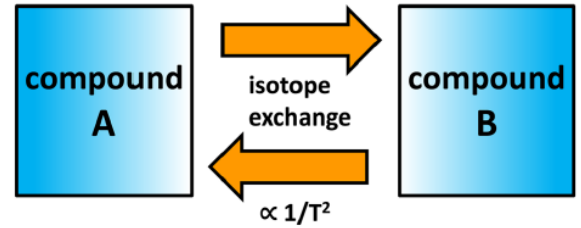

Wiederhold JG (2015) EST, **49**,2606-2624.

Rules

- The lightest isotope reacts the fastest
- The heaviest isotopes prefers the strongest bonds
- Isotope fractionation is largest for light elements and with elements having different oxidation states

$$\delta^x E = \left[\frac{\left(\frac{E^x}{E^y}\right) sample}{\left(\frac{E^x}{E^y}\right) standard} - 1 \right] * 100$$

x and y are two isotopes of the element E
x is usually the heaviest isotope

Main problem: mass bias (mass discrimination) of an ICP source

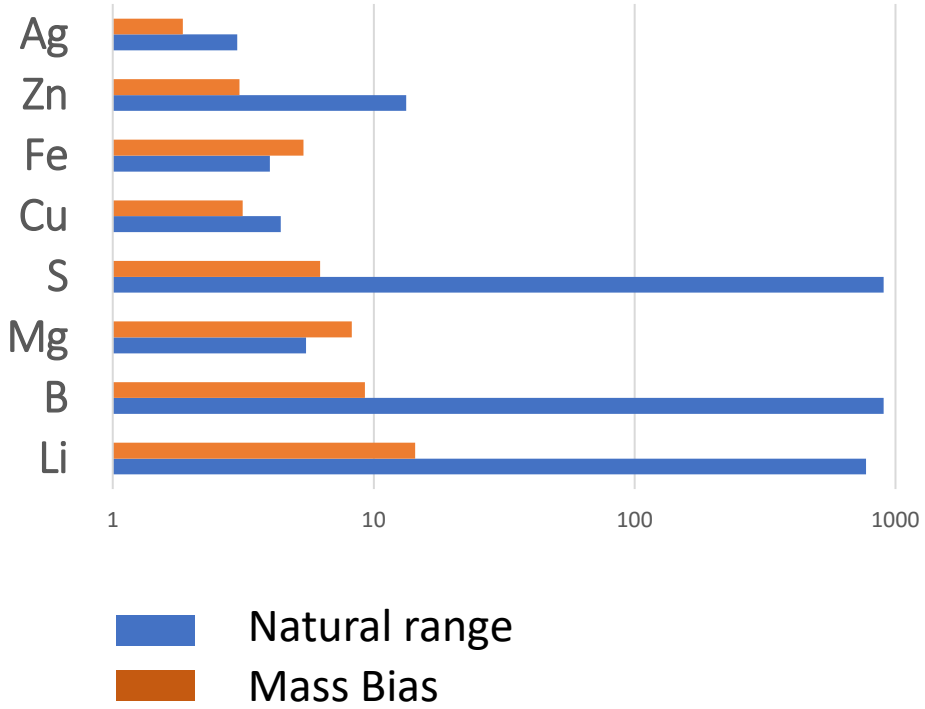

Correction methods:

- Sample-standard-bracketing

- Internal mass bias correction, using a stable isotope ratio of the same element
  Not possible unless double spike

- External mass bias correction, using a stable isotope ratio of a different element
  e.g. Zn or Ni for Cu isotopes

Cu isotopic variation in nature

$$\delta^{65}\mathrm{Cu} = [(^{65}\mathrm{Cu}/^{63}\mathrm{Cu})_{\mathrm{sample}}/(^{65}\mathrm{Cu}/^{63}\mathrm{Cu})_{\mathrm{standard}} - 1] \times 1000.$$

F. Molnár et al. / Ore Geology Reviews 77 (2016) 133–162

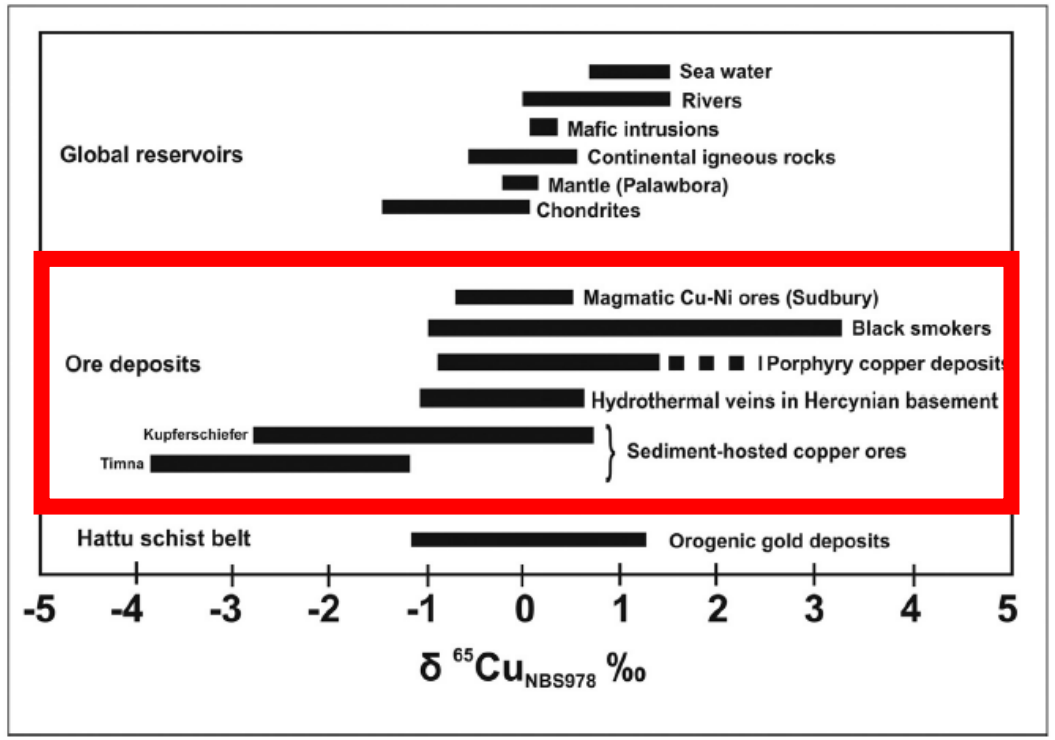

Y. Zhao et al. / Lithos 286–287 (2017) 206–215

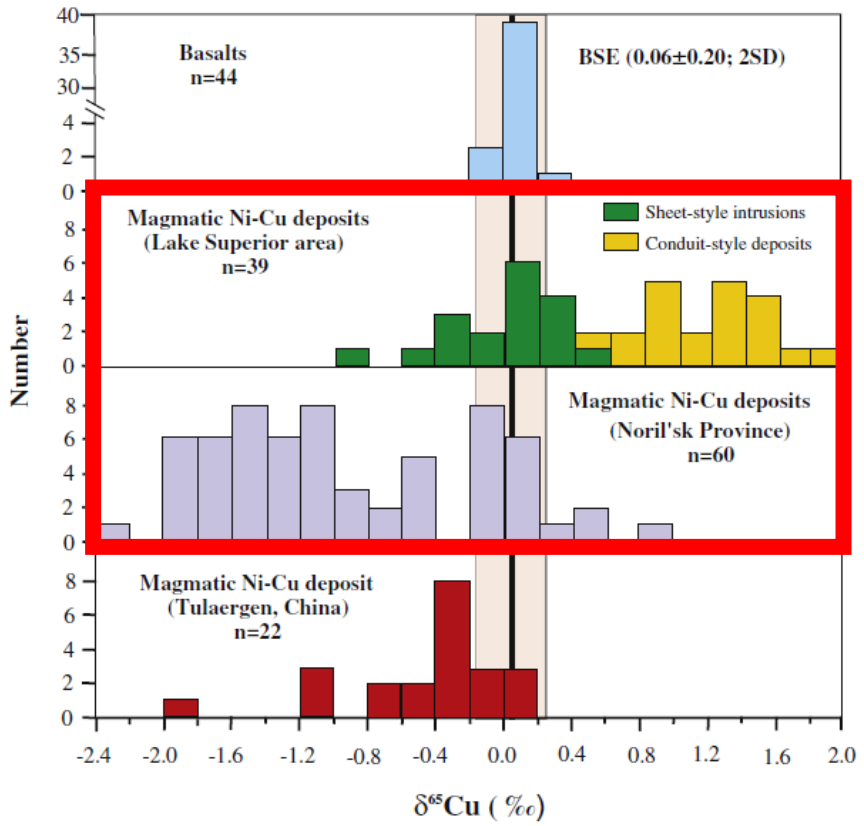

Significant Cu isotopic variations in ore deposits

Cu isotopic variations particularly large in some NiS deposits and vary according to deposit style

Solution based work

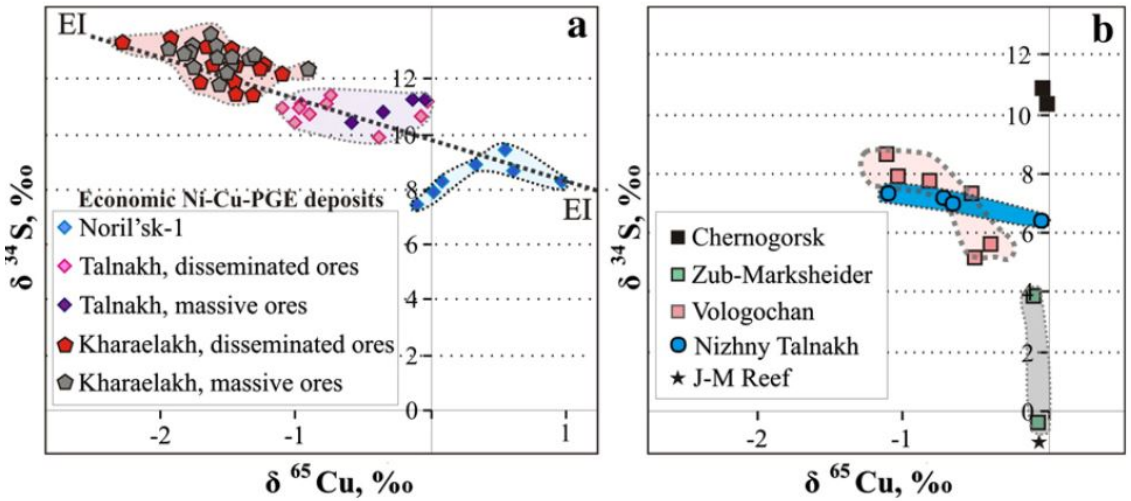

Analytical error: $\varepsilon^{65}Cu$

^{34}S–^{65}Cu systematics of Ni-Cu-PGE sulfide ores from (a) economic Kharaelakh, Talnakh and Noril'sk-1 intrusions; (b) subeconomic and non-economic intrusions of the Noril'sk Province and J-M Reef, Stillwater Complex.
Malitch et al, Lithos 204, 2014.

Laser ablation based work

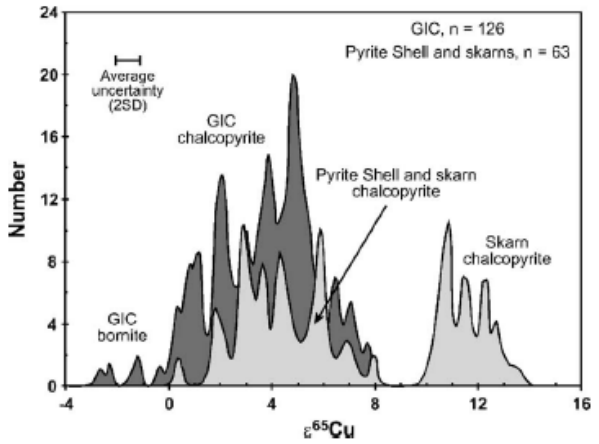

Analytical error: $\varepsilon^{65}Cu$

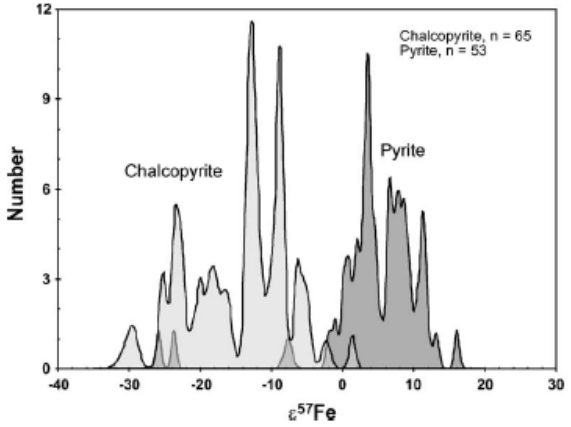

Analytical error: $\varepsilon^{57}Fe$

Tracing Cu and Fe from source to prophyry:
in situ determination of Cu and Fe ratios in sulfides From the Grasberg Cu-Au deposit,
Graham S., Peasron N. Jackson S., Griffin W., O'Reilly S.Y. Chemical Geology, 207: 147-169, 2004

$\Delta^{33}S$ isotopic variation in nature

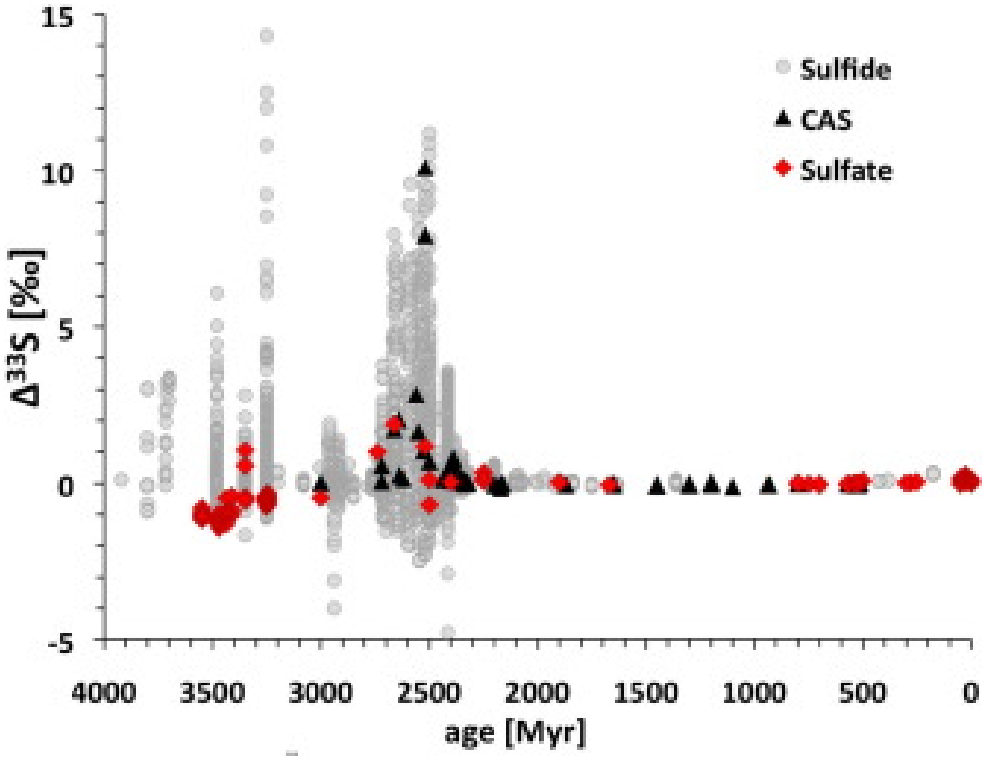

A compilation of $\Delta^{33}S$ in sedimentary sulfides (grey circles), sulfates (red diamonds), and carbonate associated sulfate (black triangles).

Claire MW et al(2014) *Geochimica et Cosmochimica Acta*, **141**,365-380

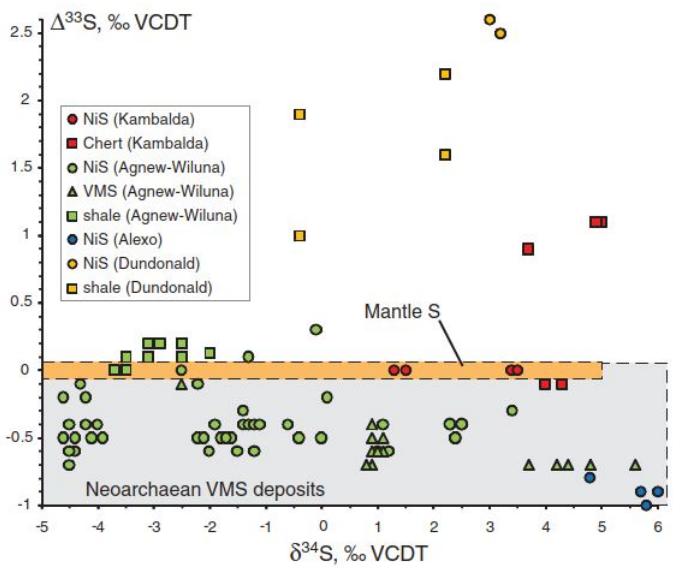

Fig. 1. $\Delta^{33}S$ versus $\delta^{34}S$ data for the studied samples and fields for mantle sulfur and Neoarchean VMS deposits. $\delta^{34}S$ values for mantle sulfur are from (*12*) and those for Neoarchean VMS deposits are from (*33*). $\Delta^{33}S$ values for the Archean mantle are inferred from (*13*, *16*) and those for the Neoarchean VMS deposits are from the current study and (*15*, *16*, *18*, *21*).

Bekker A et al(2009) *Science*, **326**,1086-1089.

$$\delta^{34}S = \left[\frac{\left(\frac{S^{34}}{S^{32}}\right)sample}{\left(\frac{S^{34}}{S^{32}}\right)standard} - 1\right] * 1000$$

$\delta^{34}S$ isotopic variation in nature

Time resolve analysis

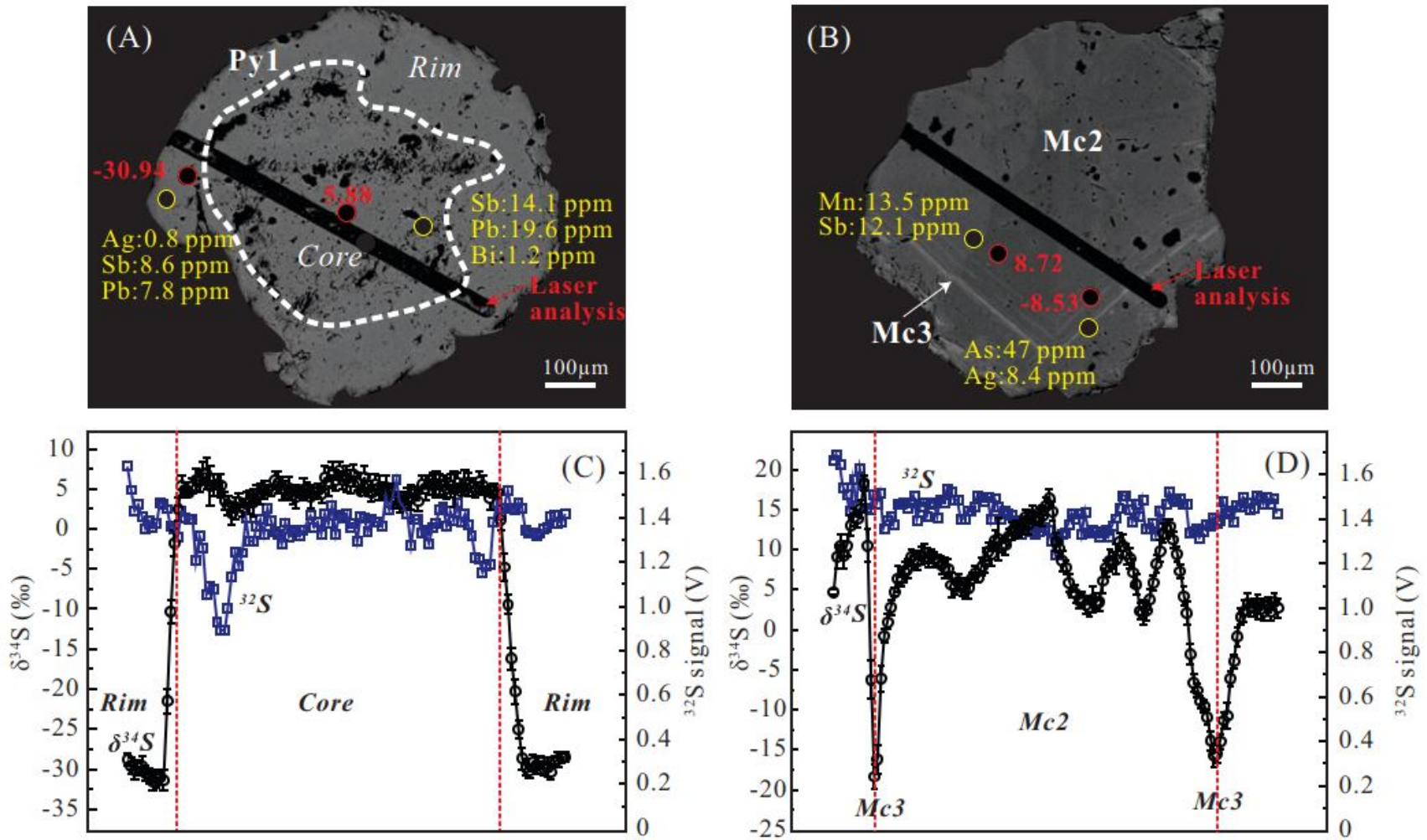

Wu Y-F, et al (2018)
Ore-Forming Processes of the Daqiao Epizonal Orogenic Gold Deposit, West Qinling Orogen, China: Constraints from Textures, Trace Elements, and Sulfur Isotopes of Pyrite and Marcasite, and Raman Spectroscopy of Carbonaceous Material. *Economic Geology*, **113**,1093-1132.

$\delta^{34}S$ isotopic variation in nature

Sample map (km scale)

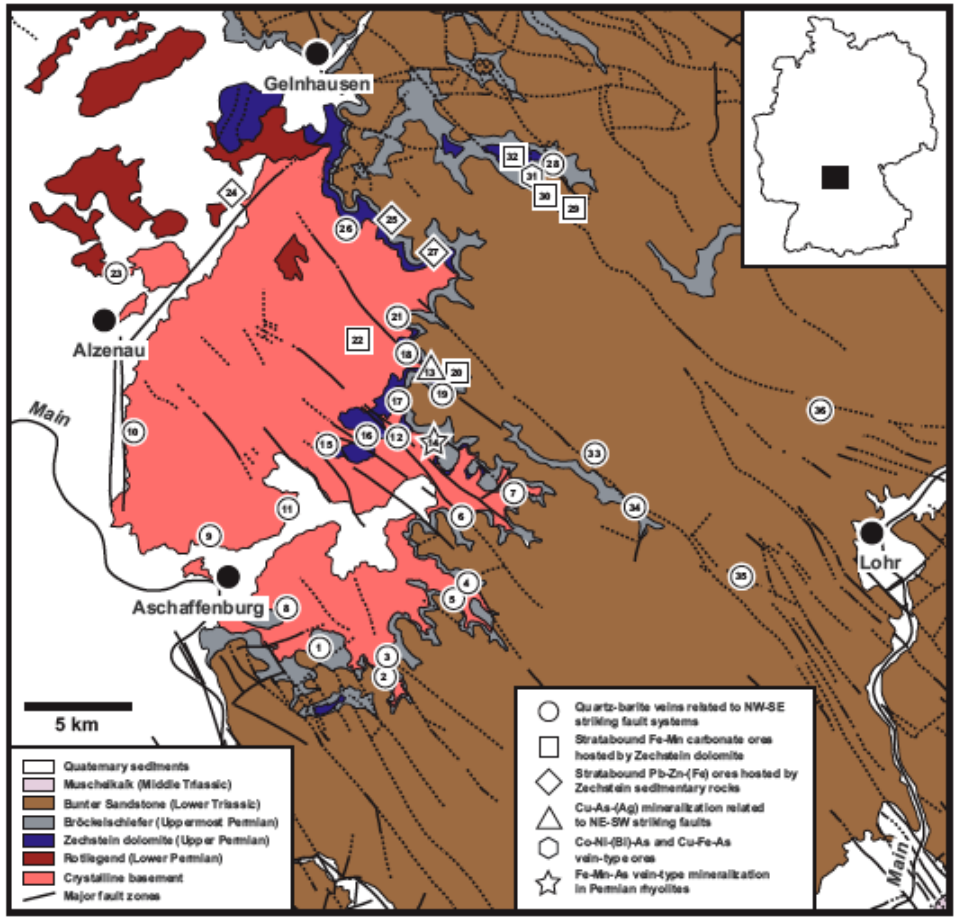

Geological sketch map of the Spessart district, showing the principal ore mineralization types and the location of the sampled deposits

Sample map (μm scale)

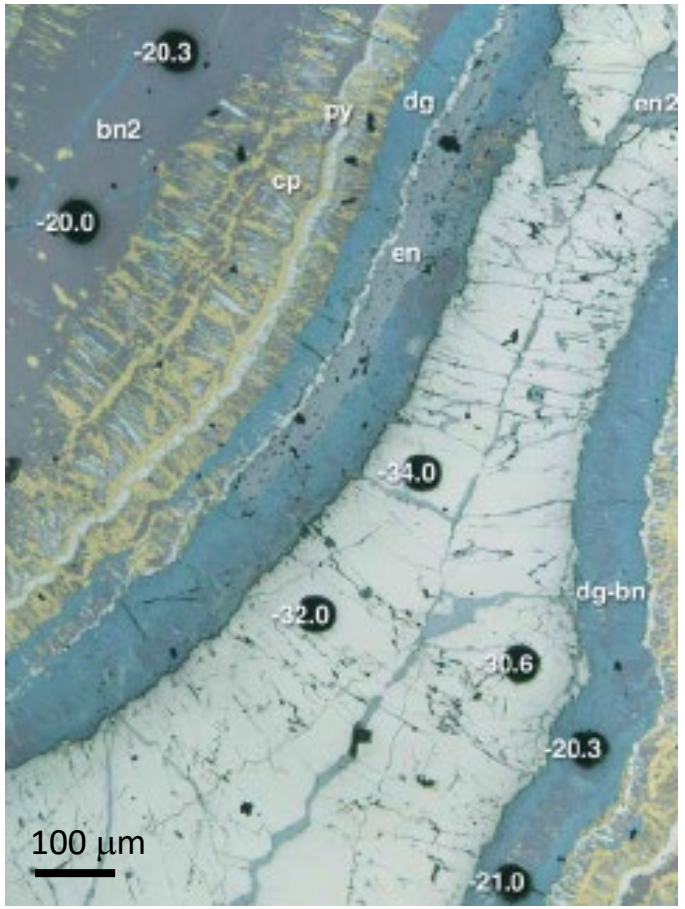

Complex intergrowth of pyrite (py), chalcopyrite (cp), bornite (bn), enargite (en) and digenite (dg)

Wagner T, et al (2010)
The role of the Kupferschiefer in the formation of hydrothermal base metal mineralization in the Spessart ore district, Germany: insight from detailed sulfur isotope studies.
Mineral Deposita, **45**,217-239.

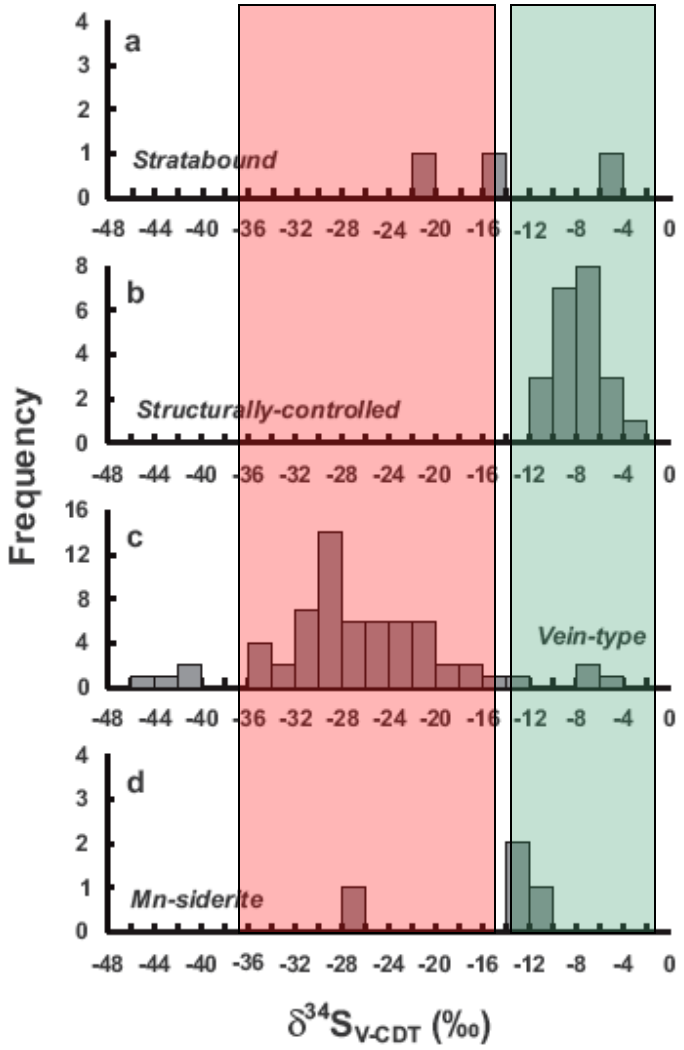

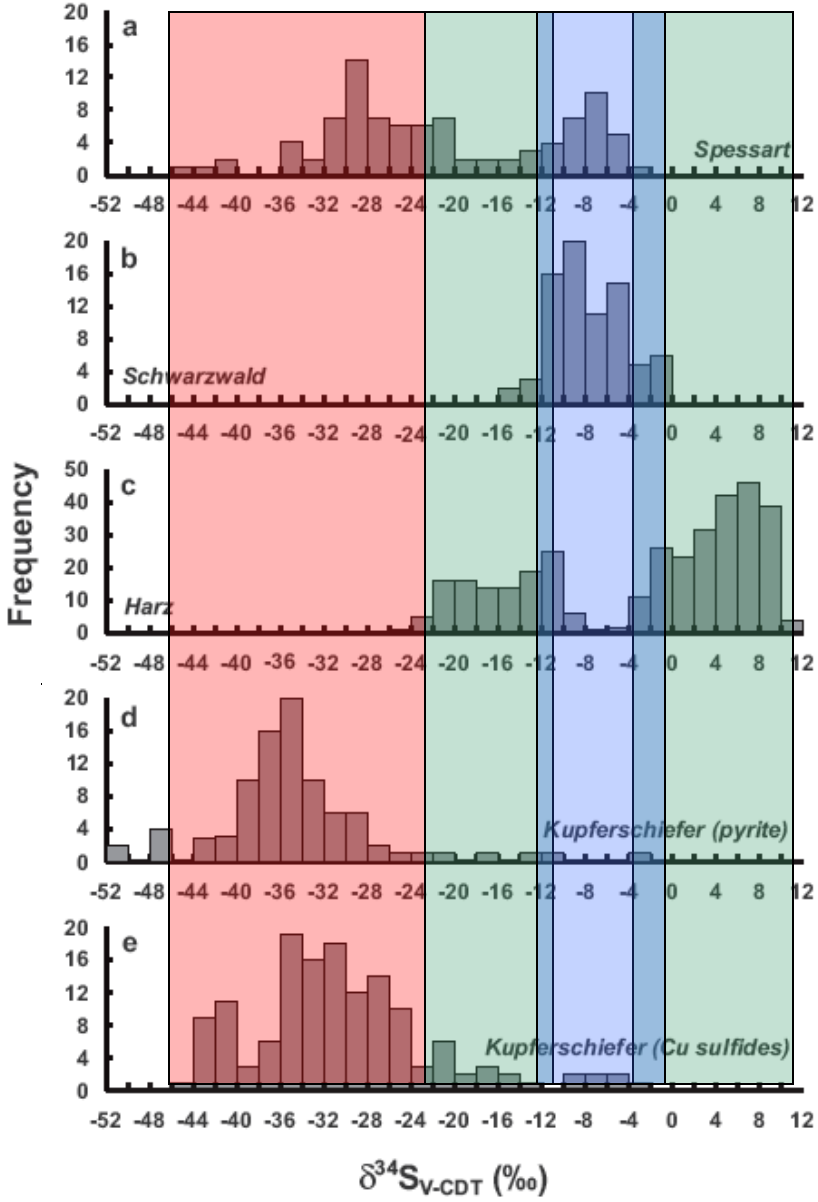

Analytical error: -

Wagner T, et al (2010)
The role of the Kupferschiefer in the formation of hydrothermal base metal mineralization in the Spessart ore district, Germany: insight from detailed sulfur isotope studies.
Mineral Deposita, **45**,217-239.

Stable isotope analysis – B isotopes on tourmaline

$$\delta^{11}B = \left[\frac{\left(\frac{B^{11}}{B^{10}}\right)sample}{\left(\frac{B^{11}}{B^{10}}\right)standard} - 1\right] * 1000$$

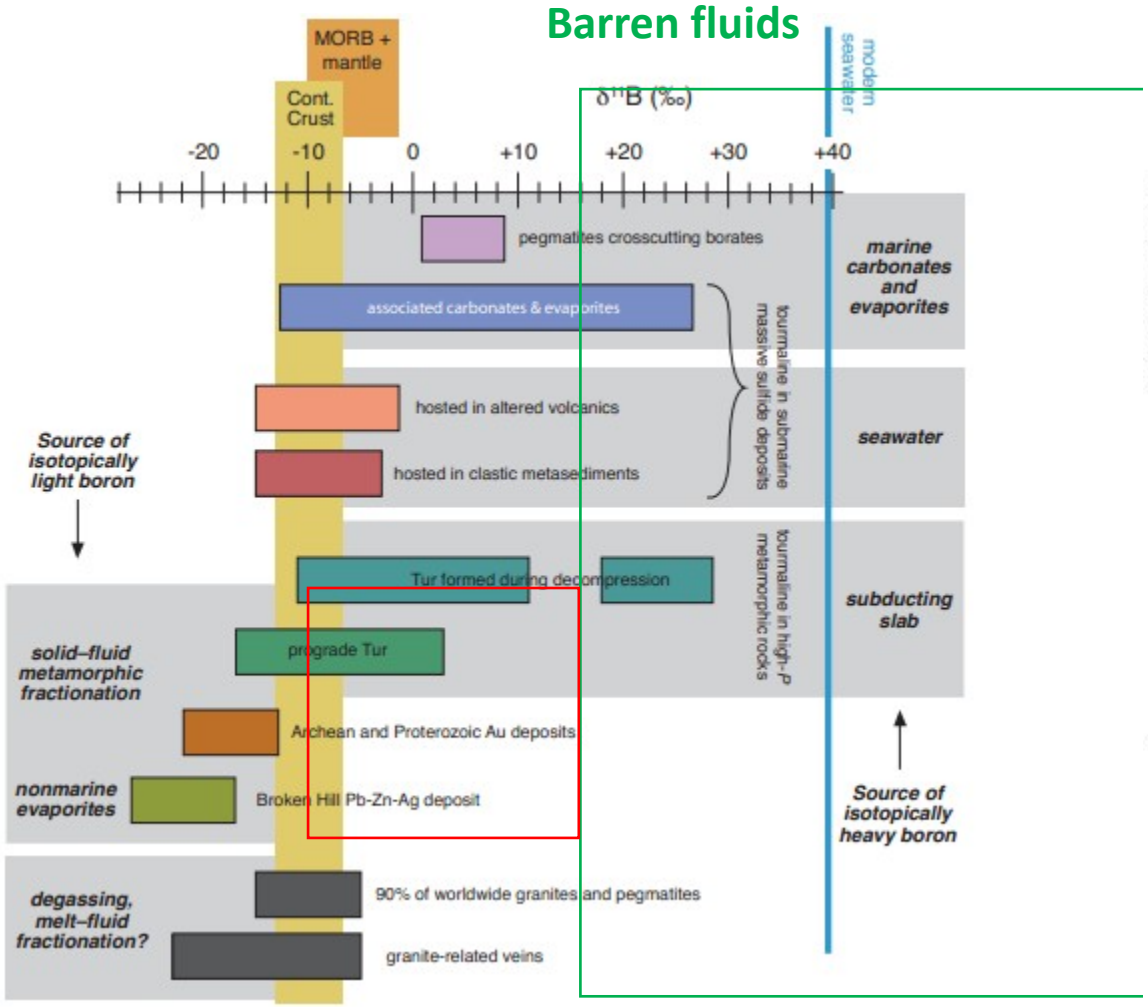

SIMS data compiled by Marschall and Jiang (2011), Elements, 7: 313-319

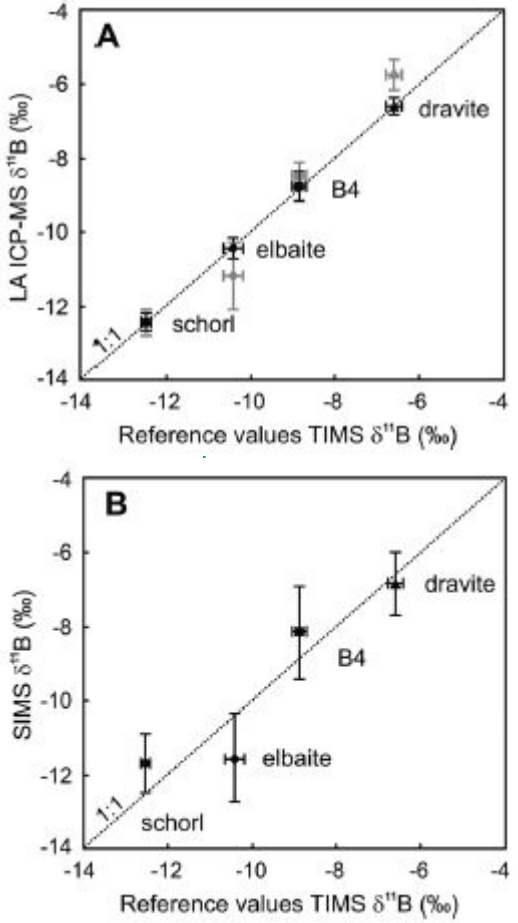

Mikova et al , JAAS, 2014

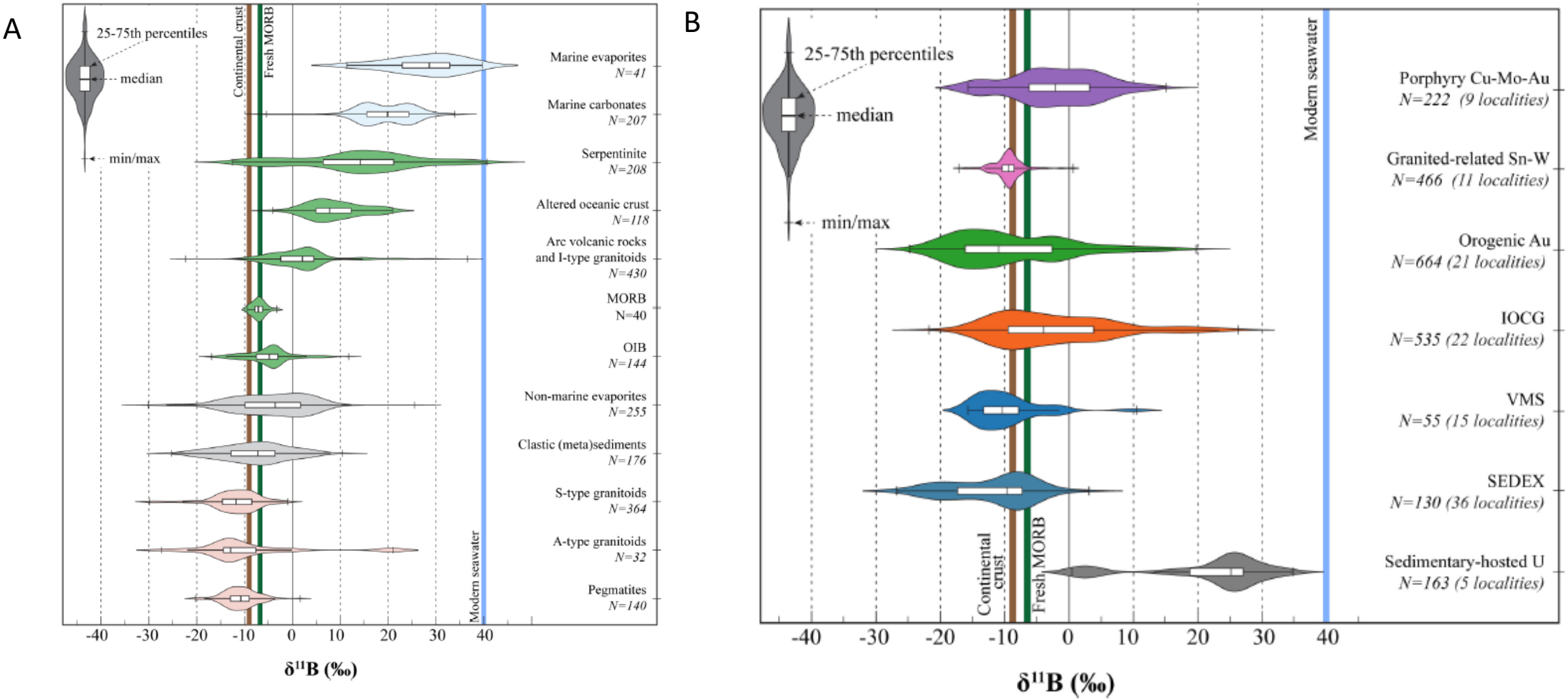

Boron isotope compositions of (A) marine and terrestrial crustal rocks; (B) from different types of hydrothermal ore deposits

Trumbull et al (2020) *Ore Geology Reviews*, **125**,103682.

Boron isotopes in tourmaline:

Daver L, Jébrak M, Beaudoin G & Trumbull RB (2020) Three-stage formation of greenstone-hosted orogenic gold deposits in the Val-d' Or mining district, Abitibi, Canada: Evidence from pyrite and tourmaline. *Ore Geology Reviews*, **120**,103449

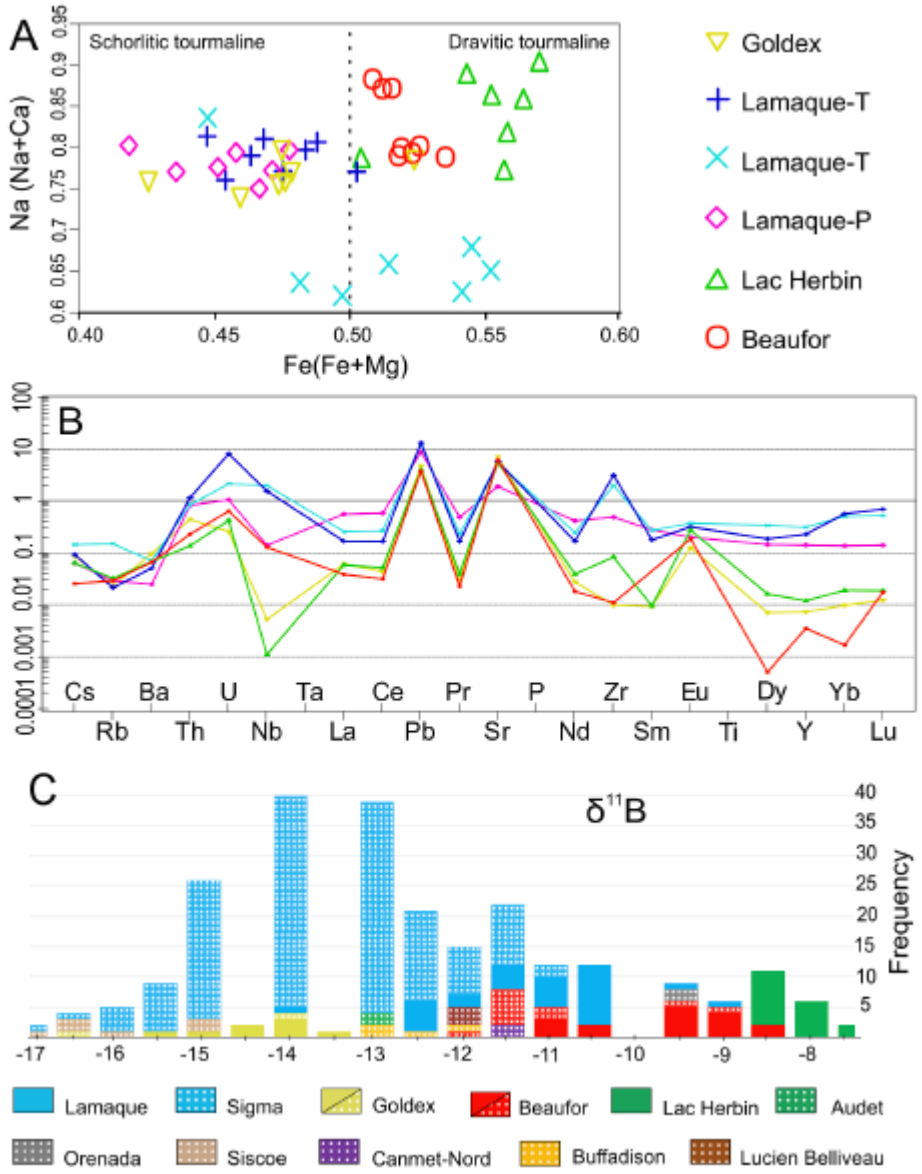

Boron isotopes in tourmaline:

Hu D-L & Jiang S-Y (2020) In-situ elemental and boron isotopic variations of tourmaline from the Maogongdong deposit in the Dahutang W-Cu ore field of northern Jiangxi Province, South China: Insights into magmatic-hydrothermal evolution. *Ore Geology Reviews*, **122**,103502.

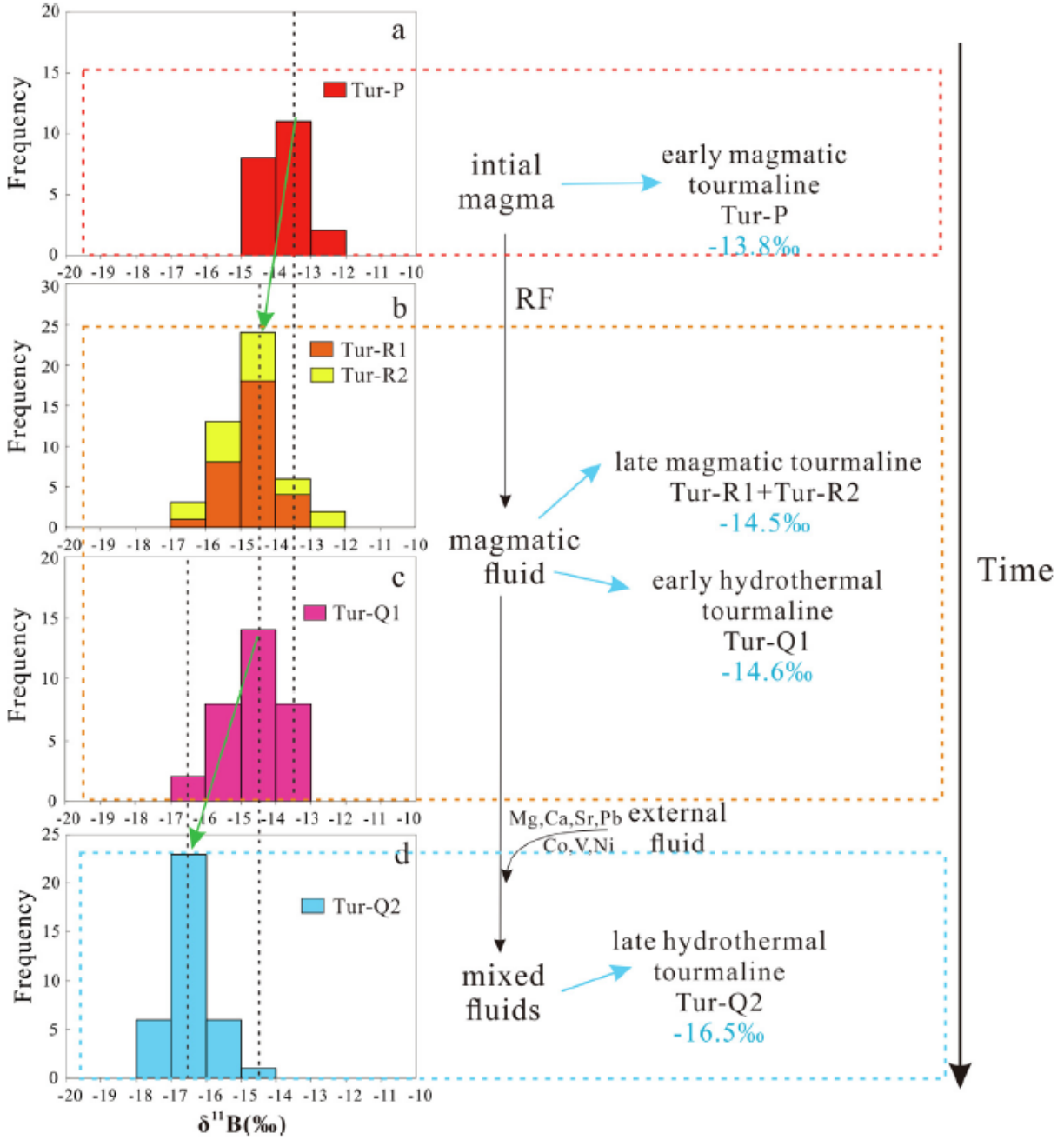

Lithium isotopes in spodumene

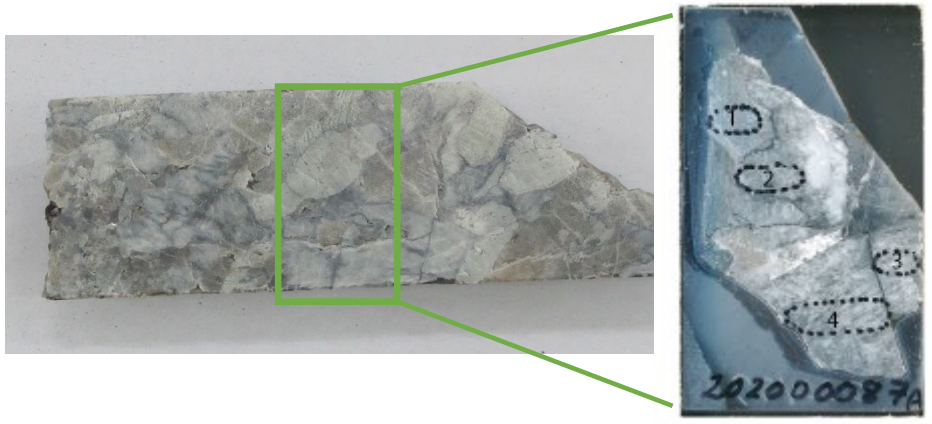

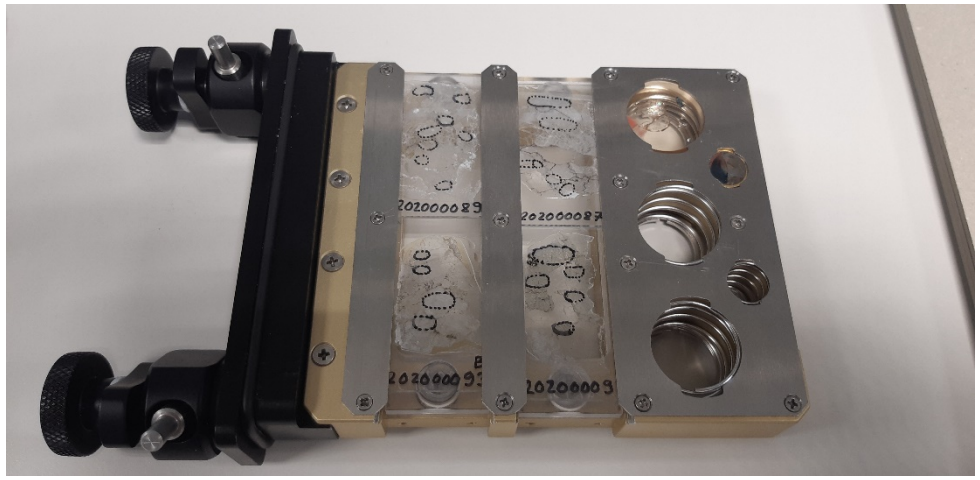

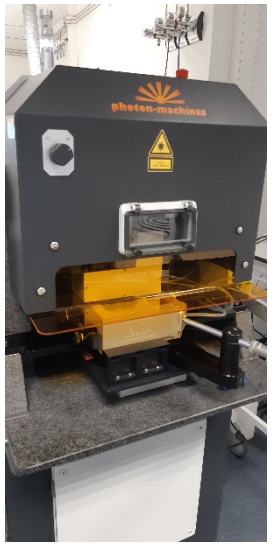

Analyzing the Li-isotopic composition from solutions is time consuming process including sample crushing, grinding and dissolution, ion exchange and the measurements.
Li isotope have been analyzed in-situ from polished sections by LA-MC-ICPMS or separated grains in epoxy mounts.

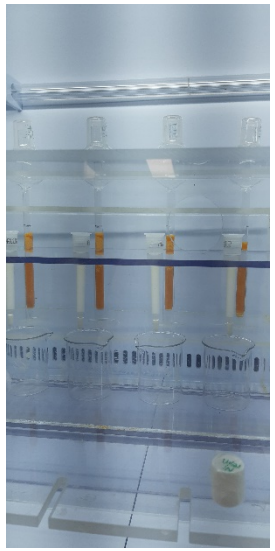

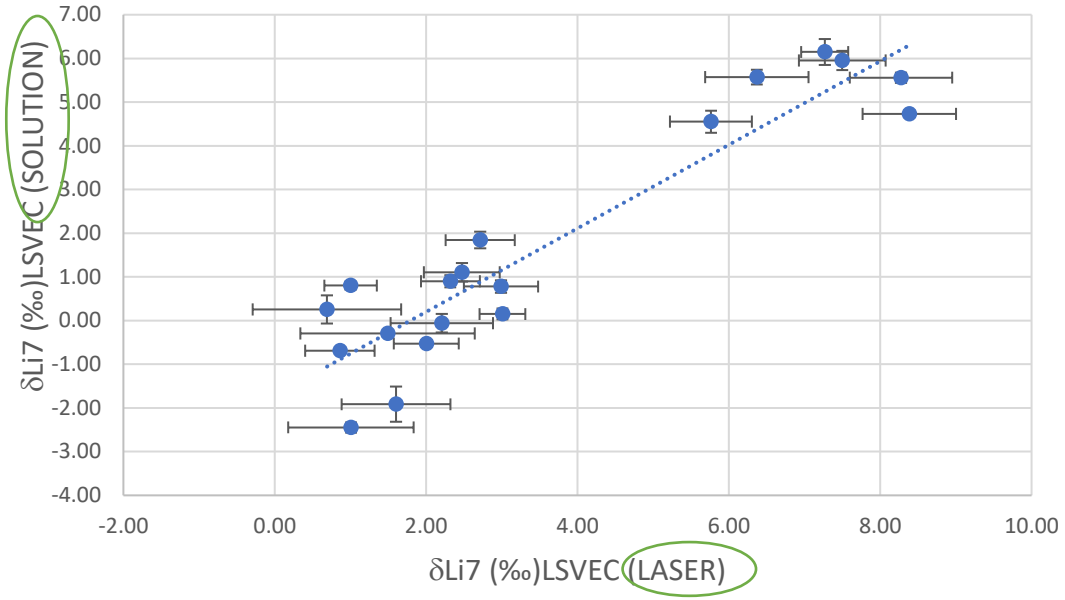

$$\delta^7 Li(‰) = \left[\frac{\left(^7Li/^6Li\right)_{unknown} - \left(^7Li/^6Li\right)_{standard}}{\left(^7Li/^6Li\right)_{standard}} \times 10^3 \right]$$

Mineral Exploration Targeting

eit RawMaterials Connecting matters

Funded by the European Union

eit RawMaterials ACADEMY

Silver

$$\delta^{109}Ag/^{107}Ag \qquad \delta^{109}Ag‰ = \left(\frac{\left(\frac{^{109}Ag}{^{107}Ag}\right) sample}{\left(\frac{^{109}Ag}{^{107}Ag}\right) NIST978} - 1 \right) * 1000$$

Standard bracketing

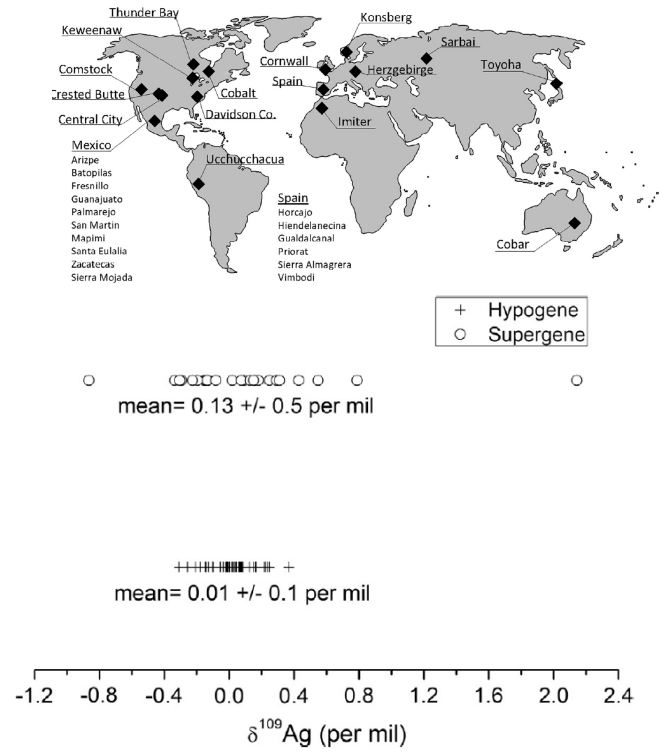

Fig. 7. Comparison of the $\delta^{109}Ag$ values for hypogene and supergene native silver specimens from around the world.

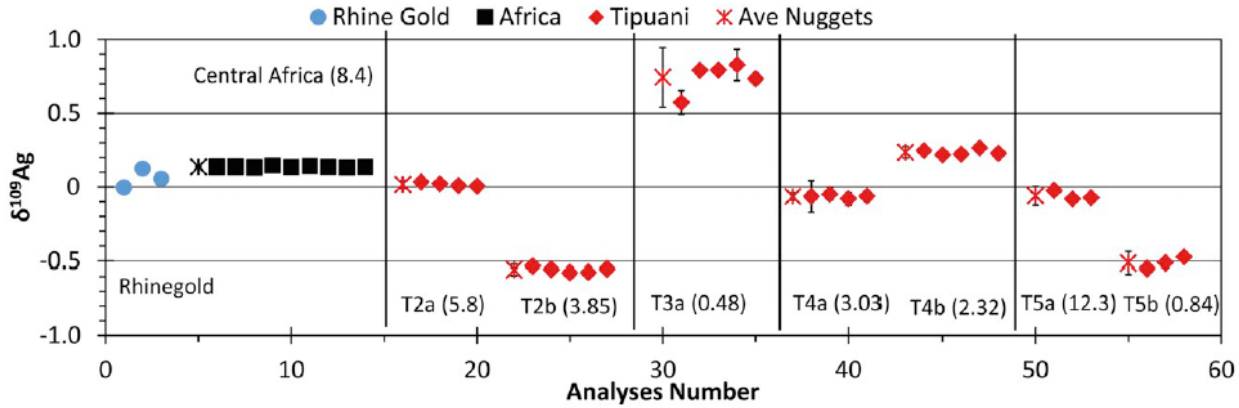

Brügmann et al.(2019) Silver isotope analysis of gold nuggets…*Chemical Geology*, **516**,59-67.

Mathur et al (2018)
Fractionation of silver isotopes in native silver explained by redox reactions.
GCA, **224**,313-326.

Gold fingerprinting

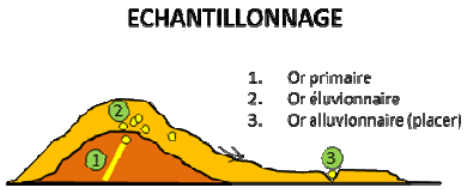

CARACTERISATION

Optique	Chimique	Isotopique
Microscopie optique Microscope électronique à balayage (MEB)	Microsonde électronique ICP/MS – Ablation laser ICP-MS sur grains mis en solution	Isotopes du Plomb
Morphoscopie des grains Identification des inclusions minérales	Chimisme des grains pour éléments majeurs et traces	Signature isotopique des grains Identification des sources

Augé et al, 2015

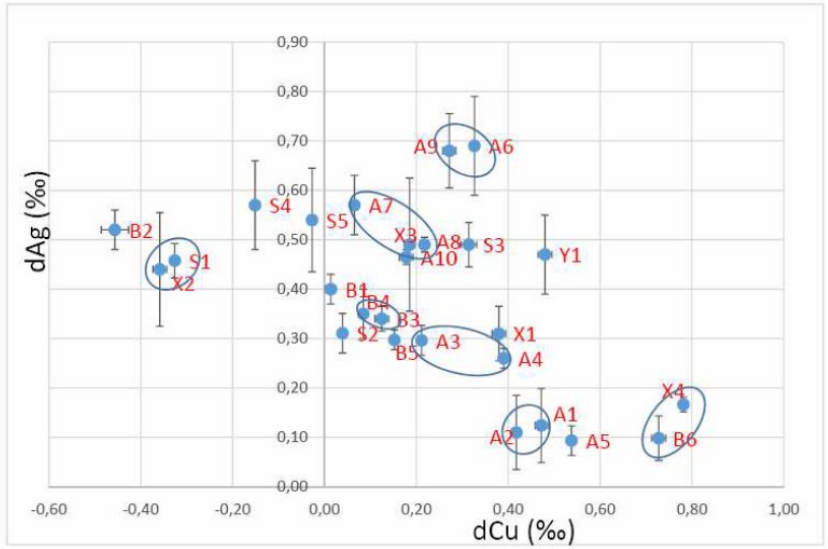

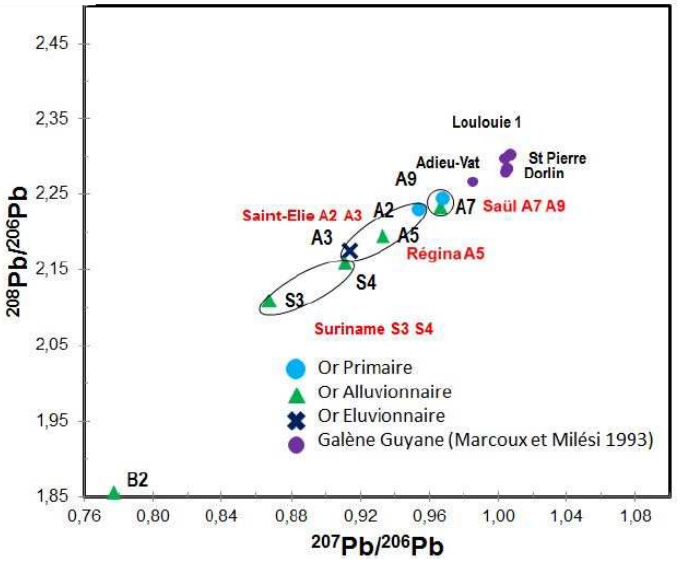

The future

- **New generation of lasers (fs)**
- **LIBS**
- **New generation of MC-ICP-MS**

  Collision cell/detectors with larger dynamic range

  New isotopic systems available for exploration

- **New technology**

  Triple quad (new geochronogical tools)

  and

  Time Of Flight (geochronology and trace elements)

- **Big data** (no isotope is a golden bullet of exploration, several isotopes, combined with geochemistry, petrography, geophysics etc…)